12-2010

Analysis of the Response of Medicago Truncatula Calcium Oxalate Mutants to Abiotic Stress

Wayra Gabriela Navia-Gine
University of Arkansas, Fayetteville

ANALYSIS OF THE RESPONSE OF *MEDICAGO TRUNCATULA* CALCIUM OXALATE MUTANTS TO ABIOTIC STRESS

ANALYSIS OF THE RESPONSE OF *MEDICAGO TRUNCATULA* CALCIUM OXALATE MUTANTS TO ABIOTIC STRESS

A thesis submitted in partial fulfillment
of the requirements for the degree of
Master of Science in Cell and Molecular Biology

By

Wayra Gabriela Navia-Giné
Universidad Autónoma Gabriel René Moreno
Bachelor of Science in Biology, 2005
University of Arkansas
Master of Science in Plant Pathology, 2007

December 2010
University of Arkansas

ABSTRACT

Calcium oxalate crystals are found in most plant species. In *Medicago truncatula* wild-type A17, crystals accumulate in leaves along the secondary veins and the only role attributed to them so far is defense against chewing insects. Calcium oxalate deficient (*cod*) mutants were isolated in *M. truncatula*; the *cod* mutants include *cod*5, which completely lack crystals in the leaves and *cod*6 that accumulates fewer and smaller crystals compared to A17. We analyzed gene expression in the *cod* mutants and A17 using GeneChip® *Medicago* Genome Arrays and found important differences in transcriptome between the three genotypes. In particular, we found a gene annotated as glyoxalase I (GLXI) referred by its tentative consensus number, TC122307, which is up-regulated in *cod*6 and down-regulated in *cod*5 as compared to constitutive levels in A17. Similarly, another *GLXI*-like gene, TC123769, is up-regulated in *cod*6 and transcripts are down-regulated in *cod*5. In previous studies, overexpression of *GLXI* has been linked to salt tolerance using transgenic approaches. Therefore, we evaluated salt tolerance in the *cod* mutants to determine if they respond differently to salt stress and if this response could be attributed to differential expression of the *GLXI*-like genes in *M. truncatula*. The *cod*6 mutant was significantly more tolerant to sodium chloride compared to A17 and *cod*5. Transcript levels of TC122307 and TC123769 do not increase in leaves following sodium chloride treatment. We also measured GLXI activity in the *cod* mutants and A17 and found no differences between genotypes. Moreover, tolerance to methylglyoxal, the substrate of GLXI, was evaluated and we found that the three genotypes were equally sensitive to toxic levels of methylglyoxal. Therefore, we conclude that TC122307 and TC123769 do not encode a functional

GLXI. Another gene, TC122323, which is more likely to encode GLXI based on sequence analysis, is constitutively expressed in the three genotypes which would explain the similar glyoxalase I activity levels in the *cod* mutants and the equal sensitivities to methylglyoxal. Overall, TC122307 and TC123769 are not likely to encode GLXI, but potentially contribute to salt tolerance in *cod*6 and encode members of the vicinal oxygen chelate enzyme superfamily. Therefore, the genes encoding these proteins are excellent candidates for further study as tools to enhance salt tolerance in crop plants.

This thesis is approved for Recommendation to the Graduate Council

Thesis Director:

_____

Dr. Kenneth L. Korth

Thesis Committee:

_____

Dr. Vibha Srivastava

_____

Dr. Ralph Henry

_____

Dr. Pengyin Chen

THESIS DUPLICATION RELEASE

I hereby authorize the University of Arkansas Libraries to duplicate this thesis when needed for research and/or scholarship.

Agreed _____

Wayra G. Navia-Giné

Refused _____

Wayra G. Navia-Giné

ACKNOWLEDGMENTS

I will be eternally thankful to my advisor for giving me the chance to work in his lab, for his patience and for trusting in me. It has been an honor to work with such a great scientist and person.

I am deeply thankful to Dr. Paul McLeod and his wife Lou McLeod; without their help I would not have been able to feel like home in the U.S. Their friendship is a treasure to me.

I would like to thank my committee members for taking their time to review this thesis and for all their suggestions. I am also very grateful to my labmates, Lacy, Faye, and Michelle.

I thank God, who gave me health to finish this work. I feel very grateful to my husband who took care of me in the hardest moments and cheer me up when I needed the most. I am also very grateful to my parents who did everything they could to give me the best education and values to be the person I am today. They showed me unconditional love and support especially during the last five years. Lastly, but not least I would like to thank my daughter who has been my inspiration and strength to accomplish each and every objective. She showed me what truly happiness is with her first smile and every single day since she came to this world. To her I dedicate this thesis.

TABLE OF CONTENTS

LIST OF FIGURES AND TABLES

INTRODUCTION

Calcium oxalate (CaOX) crystals are found in over 200 plant families and are the most abundant mineral crystals in plants (McNair, 1932). Proposed roles of CaOX crystals include plant defense against chewing insects (Korth et al., 2006), detoxification, ion balance and tissue support (Franceschi and Nakata, 2005). Although these crystals are widespread and abundant, their precise physiological role(s) and the mechanisms of their formation are not known. It is clear however, that the localization, size, and shape of CaOX crystals can be modulated by multiple genes. Calcium oxalate defective (*cod*) mutants have been isolated in the model legume *Medicago truncatula* (Nakata and McConn, 2000). These crystals are found in a sheath surrounding secondary veins in leaves of wild-type *M. truncatula* cv. Jemalong A17. The *cod* mutants that show alterations in crystal amount include *cod*5, which lacks crystals, and *cod*6 containing smaller and fewer crystals along the vascular strands when compared to wild-type A17 (Nakata and McConn, 2000). To assess differential gene expression that potentially leads to or results from the *cod* mutation phenotypes, transcriptome data were analyzed from the *cod* mutants and wild-type *M. truncatula*. The specific objectives of this research project were to: (1) analyze GeneChip® *Medicago* Genome Array data from the *cod* mutants and wild-type *M. truncatula*, (2) characterize members of the glyoxalase I-like gene family within *M. truncatula* based upon their differential expression patterns in the *cod* mutants, and (3) evaluate phenotypic and gene expression responses of *cod* mutants to salt stress. Finally, in order to take the initial steps toward

functional characterization, I produced transgene constructs of glyoxalase I-like genes from *M. truncatula* for expression in Arabidopsis.

The model legume *Medicago truncatula*

Legumes are economically important, providing grain, forage, edible oils and resources for industry. Legumes are also important for their contribution to sustainable agriculture as nitrogen-fixers in association with rhizobial bacteria. Crop legumes include soybean, alfalfa, and common bean. These crops have relatively long life cycles and large genome sizes that add complexity to research efforts and limit their usefulness as research tools. Therefore a closely related species, *Medicago truncatula* Gaertn. or 'barrel medic', has been chosen as a model legume system to be used in genetic research. A relatively short life cycle, self-pollination, small diploid genome and efficient methods for transformation have established *M. truncatula* as one of the most accepted models for legume biology (Cook, 1999).

A joint initiative to sequence the genome of *M. truncatula* began over eight years ago. Currently, the *Medicago* genome sequencing project is closer to completion with the assembly of about 90 % of all gene-rich regions (Young and Udvardi, 2009). Other genomic tools include expressed sequence tags (ESTs) available in the public database of the DFCI *Medicago truncatula* Gene Index (http://compbio.dfci.harvard.edu/cgi-bin/tgi/gimain.pl?gudb=medicago), the gene expression atlas (Benedito et al., 2008), and a wide range of mutant populations. These genomic resources have facilitated research and provided insights into growth,

development and other processes as well as interactions with other organisms (Young and Udvardi, 2009). For these reasons we chose *M. truncatula* as our plant system.

Calcium oxalate crystals

Calcium oxalate (CaOX) crystals in plants are formed in diverse shapes and sizes from environmentally derived calcium and biologically synthesized oxalate (Franceschi and Nakata, 2005). The presence of CaOX in plants has been explained as a means to regulate calcium levels and to reduce the toxic effect of oxalate to a more tolerable form (Libert and Franceschi, 1987). Although the mechanisms that control CaOX formation are unknown, the many shapes and locations of these crystals observed among multiple plant species make it evident that many factors contribute to crystal formation (Nakata and McConn, 2007). These crystals are found in well over 200 plant families and in many cases can be found in numerous tissues within the same species. Crystals of CaOX have been observed inside plant cells within the vacuoles of specialized cells called idioblasts and outside cells as well (Franceschi and Nakata, 2005). The most common forms of CaOX crystals are the raphide, styloid, prism, crystal sand, and druse (Franceschi and Horner, 1980).

Calcium oxalate crystals in *M. truncatula*

In wildtype *M. truncatula* (cv. Jemalong A17), prismatic crystals ranging from 8-10 microns in length accumulate in a sheath along the secondary vein, and smaller crystal sand forms in interveinal mesophyll cells in mature leaves. Mutants defective in CaOX formation (*cod*) were first isolated from *M. truncatula* by screening an ethyl

methanesulfonate (EMS)-mutagenized population (Nakata and McConn, 2000), and show alterations in crystal number and shape. For example, significantly fewer crystals along the vascular strands are found in *cod*6 when compared to A17, and *cod*5 does not accumulate any crystals along vascular strands. Each mutant was crossed with A17 and the progeny resulted in wild-type crystal patterns, demonstrating that these *cod* phenotypes are due to a recessive mutation. In addition, the *cod*5 and *cod*6 lines were crossed with each other and the ensuing progeny display a wild-type crystal phenotype, indicating that the mutant phenotypes result from non-allelic mutations (Nakata and McConn, 2000). The *cod*5 mutant has been used to investigate the importance of crystal formation in plant growth and development. Nakata and McConn (2003) found that *cod*5 displayed similar growth habits as wild-type controls, suggesting that CaOX crystal formation does not play a critical role in plant growth and development in *M. truncatula* grown within a controlled environment. Moreover, four additional mutants containing increased CaOX druse crystals within mesophyll cells were identified in *M. truncatula*. These mutants were designated mesophyll oxalate defective (*mod*), and a genetic analysis showed that the druse crystal accumulation in each mutant is due to a single mutation at different loci; again indicating that multiple loci affect the accumulation and localization of CaOX crystals (Nakata and McConn, 2007).

Plant responses to salt stress

Plants have evolved complex signaling pathways to cope with abiotic stresses such as drought, salinity, osmotic stress and cold. These environmental factors are major causes of crop yield decreases worldwide, leading to losses of billions of dollars

per year (Pitman and Läuchli, 2004). Soil salinity can be a result of use of saline water for irrigation, poor drainage, excessive and unnecessary fertilizer applications and other factors (Bernstein, 1975). Salinity occurs particularly in arid and semiarid regions and causes a decrease in plant growth as well as necrotic leaf symptoms (Bernstein, 1975). Shoot growth is generally more affected than root growth, although roots are exposed directly to salt (Bernstein, 1975). Plants under salt stress also develop chlorosis due to the decrease of chlorophyll content (Hernández et al., 1995). Salt-induced symptoms are originally caused by the disruption of osmotic and ionic homeostasis, which leads to water deficit and damage of proteins and membranes (Bernstein and Hayward, 1958; Vinocur and Altman, 2005). The response to salt stress will vary depending on the stage of development; salt-tolerant plants usually adapt gradually to salinity as they grow older (Bernstein and Hayward, 1958). In addition, differential response to salt stress has been observed within a species at certain developmental stages. For example, 35 alfalfa cultivars responded differently to salt stress at the seedling stage (Al-Khatib et al., 1993). Moreover, germination can often occur once salt conditions diminish, as is the case of sugar beet seed (Bernstein and Hayward, 1958). In general, stage of development and nature of the crop influence the degree of salt tolerance.

Strategies to increase salt tolerance in economically important plants include the selection of plants under high salt conditions with subsequent breeding techniques and marker-assisted selection (Yamaguchi and Blumwald, 2005). Other possible alternatives are to manipulate regulation of stress-related genes or to introduce novel genes by genetic engineering (Wang et al., 2003). As an example, transgenic tomato plants overexpressing a vacuolar Na^+/H^+ antiporter protein were generated and were

able to produce fruit under salt-stress conditions, demonstrating that the alteration in regulation of a single gene is sufficient to enhance salt tolerance (Zhang and Blumwald, 2001).

During salt stress, osmotic effects cause water deficit which leads to the formation of reactive oxygen species (ROS), such as hydrogen peroxide (H_2O_2), superoxide ($O_2^{\bullet -}$), hydroxyl radical ($^{\bullet}OH$), and singlet oxygen ($^1O_2$) (Parida and Das, 2005). Therefore, another approach to increase salt tolerance is to manipulate the regulation of genes involved in the production of antioxidants to reduce stress-induced ROS (Vinocur and Altman, 2005). For example, the *AtALDH3* gene encoding an aldehyde dehydrogenase was overexpressed in *Arabidopsis thaliana* (Arabidopsis) resulting in higher tolerance to salt and drought stress. The *AtALDH3* gene product catalyzes the oxidation of toxic aldehydes produced by ROS reacting with lipids and proteins (Sunkar et al., 2003).

Medicago truncatula is a salt-sensitive species (glycophyte) and is adapted to different environmental conditions; therefore it is a good model to understand salt stress responses in legumes (Merchan et al., 2007). A study examined the mean shoot biomass of *M. truncatula* accessions under saline conditions and showed very few differences, indicating that there is similar response to salt stress among accessions (Veatch et al., 2004). In an attempt to increase salt tolerance in *M. truncatula*, transgenic plants overexpressing the Δ^1-pyrroline-5-carboxylate synthetase (*P5CS*) gene from *Vigna aconitifolia* were generated. These plants accumulate higher proline levels that enhance osmotolerance, and ultimately display nitrogen-fixing activity, a desirable attribute of legumes (Verdoy et al., 2006). A leucine-rich repeat receptor-like kinase

(RLK), namely *Srlk*, induced in root tissue by salt stress was identified in *M. truncatula*. An RNAi approach revealed that decreased *Srlk* expression prevents inhibition of root growth during salt stress conditions. In addition, gene expression analysis showed that salt-responsive genes were down-regulated in the *Srlk*-RNAi roots under salt conditions, suggesting that *Srlk* is involved in the regulation of early response to salt stress in roots by modulating expression of salt-responsive genes (de Lorenzo et al., 2009). These studies suggest that the identification of genes responsible for salt tolerance or involved in the regulation of adaptation and their manipulation is an excellent approach to generate plants that are salt-tolerant.

The glyoxalase system

Glyoxalase I is ubiquitous in nature and its primary function has been associated with the detoxification of methylglyoxal (MG), which is a toxic 2-oxo-aldehyde by-product of glycolysis and threonine degradation (Yadav et al., 2005a). Methylglyoxal accumulates under several stress conditions and is degraded by the glyoxalase detoxifying system that consists of two enzymes; glyoxalase I (EC 4.4.1.5, lactoylglutathione lyase) and II (EC 3.1.2.6, hydroxyacylglutathione hydrolase) (Thornalley, 1990; Yadav et al., 2005a). Glyoxalase I (GLXI) utilizes an intermediate hemithioacetal formed from MG and reduced glutathione in a non-enzymatic reaction and converts it into *S*-D-lactoylglutathione. Glyoxalase II (GLXII) catalyzes the hydrolysis of *S*-D-lactoylglutathione to D-lactic acid with the regeneration of reduced glutathione (Fig. 1) (Thornalley, 1990).

Glyoxalase I has been purified and studied in several organisms, such as *Saccharomyces cerevisiae* (Inoue et al., 1998) and *Homo sapiens* (Aronsson et al., 1979). In plants, GLXI has been characterized in *Glycine max* (Skipsey et al., 2000), *Lycopersicum esculentum* (Espartero et al., 1995), *Brassica juncea* (Veena et al., 1999), and most recently in *Triticum aestivum* (Lin et al., 2010). Previous studies suggest that GLXI plays a regulatory role in cell division in plants. In *Datura* callus, GLXI activity correlates with cell proliferation in presence of spermidine, a growth stimulant; however activity is inhibited by vinblastine and MG, inhibitors of cell division (Ramaswamy et al., 1984). Glyoxalase I was also studied in *Brassica oleracea* where cell proliferation was reduced in the presence of calmodulin inhibitors, which caused a decrease in GLXI activity (Bagga et al., 1987). In callus cultures of *Amaranthus paniculatus*, cell proliferation increased under blue light stimulation, which consequently caused an increase in GLXI activity (Chakravarty and Sopory, 1998). These studies show that the function of GLXI is associated with cell division and proliferation, although the causal relationship has not yet been established.

The glyoxalase system in stress response

Several reports revealed that *GLXI* transcripts increase during stress response in plants. Sodium chloride and mannitol application caused an increase in transcript accumulation of *GLXI* in *L. esculentum* (tomato), reaching higher accumulation after 72 h of treatment (Espartero et al., 1995). In *T. aestivum* (wheat), the gene encoding GLXI, designated *TaGlyI*, was induced by the fungal pathogen *Fusarium graminearum*, NaCl and $ZnCl_2$ (Lin et al., 2010). It has been also shown that MG levels increase in

leaves and roots of *Oriza sativa*, *Pennisetum glaucum*, *N. tabacum*, and *B. juncea* under salinity stress (Yadav et al., 2005a). Transgenic tobacco plants overexpressing *GLXI* from *B. juncea* in sense orientation showed significant tolerance to NaCl compared with wild-type plants, as indicated by higher chlorophyll content (Veena, 1999). Double transgenic tobacco plants overexpressing *GLXI* from *B. juncea* and *GLXII* from *O. sativa* also resulted in enhanced salinity tolerance (Singla-Pareek et al., 2003). The same transgenic plants display tolerance to high $ZnCl_2$ levels and are able to produce viable seeds indicating that the glyoxalase system can provide protection to Zn^{2+} toxicity in addition to NaCl stress (Singla-Pareek et al., 2006). The overexpression of *GLXII* alone also proved to be effective to rescue rice from toxic levels of MG and NaCl (Singla-Pareek et al., 2008). In addition, *GLXI* from *B. juncea* was introduced into Arabidopsis under the control of the salt-inducible promoter rd29, and this conferred tolerance to 150 mM NaCl (Roy et al., 2008). Even in a non-plant organism, *S. cerevisiae*, *GLXI* was found to be up-regulated by NaCl corresponding to an increase in enzyme activity, indicating that GLXI plays a role during adaptation of osmotic stress in yeast (Inoue et al., 1998).

The role of the glyoxalase system during stress was also investigated in the nematode *Onchocerca volvulus*, in which transcript levels of *GLXI* increased 3.2 fold in response to oxidative stress triggered by xanthine/xanthine oxidase and 1.95-fold in response to plumbagin (Sommer et al., 2001).

The role of glyoxalase system in disease processes has also been studied. Transcripts encoding *GLXI* and *GLXII* display a concomitant increase with GLXI and GLXII activity in human breast cancer tissue compared to normal tissue (Rulli et al.,

2001). In addition, *GLXI* was up-regulated in P301L mutant tau transgenic mice, which develop Alzheimer's disease, suggesting a role of *GLXI* in this disease (Chen et al., 2004). It was also suggested that the glyoxalase system is involved in the development of diabetic complications; as shown by an increase in glyoxalase metabolites in blood samples of diabetic patients (McLellan et al., 1994). Together, these studies show the relevance of the glyoxalase system in disease and stress conditions in a wide variety of species (Thornalley, 1990).

The vicinal oxygen chelate (VOC) enzyme superfamily

Glyoxalase I is a member of the vicinal oxygen chelate (VOC) enzyme superfamily and catalyzes an isomerization reaction (Armstrong, 2000). Members of the VOC superfamily catalyze different types of reactions; however they share a common structural scaffold and use distinct metal ions for catalysis (Babbitt and Gerlt, 1997). The main characteristic of this superfamily is a pair of βαβββ motifs that form the metal-binding active site (Armstrong, 2000). The reactions of the members of this family stabilize a transitional state containing vicinal anionic oxygen atoms, catalyzing reactions of epimerization, oxidative cleavage of C-C bonds and nucleophilic opening of epoxide (Armstrong, 2000).

Most DNA sequence data deposited in public databases is annotated based on computational analysis; therefore the majority of predicted protein sequences are not experimentally characterized. A recent study by Schnoes et al. (2009), analyzed the level of misannotation in public protein sequence databases. The study found that the VOC enzyme superfamily has a high level of misannotation in three databases:

GenBank NR, UniProtKB/TrEMBL, and Kyoto Encyclopedia of Genes and Genomes (KEGG). The level of misannotation ranged from around 25 % to over 60 %. Other families analyzed that had a high level of misannotation are enolase, haloacid dehalogenase and terpene cyclase amidohydrolase. The database with the lowest level of misannotation, close to zero, was the manually curated Swiss-Prot (Schnoes et al., 2009). An example of misannotation in the VOC superfamily is a sequence from soybean annotated as GLXI (accession no. CAA48717). In the same organism the authentic GLXI (accession no. CAA09177) has been experimentally characterized and the protein encoded by sequence CAA48717 was found to be a glutathione transferase (Skipsey et al., 2000; Schnoes et al., 2009). Another example of misannotation is the Arabidopsis *At1g07645* which is also annotated as GLXI. The Arabidopsis gene (*At1g07645*) is an orthologue of the recently characterized *Xhdsi-1*^{VOC} from *Xerophyta humilis*, both genes encode a protein that lacks the conserved glutathione and zinc binding sites which are required for activity in GLXI (Mulako et al., 2008). Moreover, overexpression of *Xhdsi-1*^{VOC} in *E. coli* failed to increase tolerance to MG and expression of this gene failed to rescue yeast carrying a mutation in *GLXI* (Mulako et al., 2008). Evidence showed that the *Xhdsi-1*^{VOC} and *At1g07645* genes encode novel members of the VOC superfamily (Mulako et al., 2008). These studies demonstrate that misannotation is not uncommon in the VOC superfamily; therefore the genes annotated as *GLXI* in *M. truncatula* should be characterized with this caveat in mind.

GeneChip® Medicago Genome Arrays were used to identify genes differentially regulated in the *cod* mutants. We found a glyoxalase I-like gene (TC122307) that is highly expressed in *cod*6 and down-regulated in *cod*5, as compared to expression levels

observed in the wild-type parental line A17. Overexpression of glyoxalase I (*GLXI*) from *Brassica juncea* increases tolerance to sodium chloride (NaCl) and methylglyoxal in transgenic tobacco, indicating that *GLXI* confers tolerance to plants under salt stress (Veena et al., 1999). Thus, we evaluated the response of the *cod* mutants to salinity to determine if the protein encoded by TC122307 potentially contributes to salt tolerance in *M. truncatula*. To further analyze the role of this gene during salt stress, we analyzed transcript levels of TC122307 and another *GLXI*-like gene (TC123769). Finally, we evaluated GLXI activity and tolerance to methylglyoxal in the *cod* mutants to determine whether up-regulation of *GLXI* genes in *cod*6 could increase GLXI activity and tolerance to methylglyoxal compared to *cod*5. We produced transgene constructs of glyoxalase I-like genes of *M. truncatula* to transform Arabidopsis. The production of these transgenic lines will help to evaluate the role of these genes in salt tolerance.

MATERIALS AND METHODS

Plant material and growth conditions

Medicago truncatula cv. Jemalong line A17, *cod*5 and *cod*6 were maintained in a growth chamber under controlled conditions of 22ºC with a 12-hour photoperiod and a photosynthetic photon flux of 170 µmol m^{-2} s^{-1}. Plants were fertilized with water-soluble tomato plant food, Miracle-Gro® every two weeks and Gnatrol® (Valent USA Corporation) was applied as biological larvicide control at the same intervals.

GeneChip® array data analysis

The sequence information in the GeneChip® Medicago Genome Arrays was obtained from The Institute for Genomic Research (TIGR) *M. truncatula* gene index and gene predictions from genome sequence by the International Medicago Genome Annotation Group (IMGAG) (http://affymetrix.com). Total RNA taken from fully expanded leaves of eight-week-old A17, *cod*5, and *cod*6 plants was submitted to the DNA Analysis Core Lab at the Dana Farber Cancer Institute and analyzed via Affymetrix Medicago Genome Array GeneChips; each plant genotype was analyzed with three independent biological replicates (K. Korth, unpublished).

In order to classify probe sets in the Affymetrix *M. truncatula* genome array and to retrieve the description of the best match sequence in the GenBank, we used the GeneBins database (http://bioinfoserver.rsbs.anu.edu.au/utils/GeneBins/). With the information obtained we made a list of differentially expressed genes from three

pairwise comparisons (*cod*5 vs. A17, *cod*6 vs. A17, and *cod*6 vs. *cod*5) with their tentative annotation and probable biological function.

Heat maps were created with Nexus expression version 1.0 (http://www.biodiscovery.com) in which A17 was compared to each *cod* mutant line. Differentially regulated genes were identified using a *P*-value threshold of 0.05 and a log-ratio threshold of 0.1.

Salt treatments

For the long-term experiments one-month-old plants were transferred to river sand and allowed to establish for a week. For treatments, solutions were applied from the bottom via flooding, and allowed to saturate the sand medium for one hour and then drained. Initial treatment started with lower concentration of sodium chloride (50 mM) and calcium chloride (25 mM) for the first 24 h. We increased the concentration to 100 mM sodium chloride and 50 mM calcium chloride at the second treatment and continued with these concentrations until the plants showed early signs of desiccation and the experiment was terminated when salt-stress symptoms were evident, about 4 weeks after initial application of salt solutions. Salt stress symptoms were evaluated visually at the end of the experiment. Sodium chloride-treated plants were phenotypically rated using a scale from 1 to 6, based on a scale by Valencia et al. (2008); 1 assigned to healthy plant with no chlorosis, 2 for 25 % of leaf chlorosis, 3 for 50 % of leaf chlorosis, 4 for 75 % of leaf chlorosis, 5 for 100 % chlorosis, and 6 for plant death and complete leaf necrosis (Fig.8).

In addition, a SPAD meter (Konica Minolta Holdings, Inc.) was used to quantify chlorophyll content in leaves. The average of fifteen measurements per plant was recorded for data analysis. For dry weight determination, aerial parts of each plant were collected and dried at 50 ˚C for 24 hours.

Mineral analysis

Chloride was analyzed on a Spectro Ciros Inductively Coupled Plasma (ICP). The plant tissue was dried and ground. A 0.1 g-sample was extracted with 30 ml distilled water and filtered. The wavelength used was 134.724 (Kalra, 1998).

Calcium and sodium were analyzed using a wet ash procedure and nitric acid (HNO_3) digestion. We used 0.25g/25ml total volume (Plank, 1992). Analysis was performed on a Spectro Arcos ICP; calcium wavelength is 315.887 and sodium is 589.592. An external check sample was used to verify results.

Phylogenetic analysis

Predicted amino acid sequences of characterized GLXI were obtained from GenBank (http://www.ncbi.nlm.nih.gov/genbank/). We searched for genes in *M. truncatula* with high similarity to *Glycine max* glyoxalase I (*GmGlxI*) using BLAST (http://blast.ncbi.nlm.nih.gov/Blast.cgi). The multiple sequence alignment was generated with Clustal W (1.81) from Biology WorkBench (http://workbench.sdsc.edu/) and the secondary structure prediction with PSIPRED (Bryson et al., 2005). The phylogenetic tree was drawn via the neighbor-joining method using Geneious Basic 5.0.3 (Drummond et al., 2010).

Primer design

Oligonucleotide primers designed for polymerase chain reaction (PCR) were analyzed for possible hairpins and primer dimers using OligoAnalyzer 3.1 from Integrated DNA Technology (http://www.idtdna.com/analyzer/Applications/ OligoAnalyzer/). The melting temperature differences between each pair were not greater than 3˚C.

RNA extraction and cDNA synthesis

Plant material was collected and immediately frozen in liquid nitrogen. Total RNA was extracted using TriReagent (Molecular Research Center, Inc. Cincinnati, OH) as indicated in the manufacturer's protocol and solubilized in DEPC-treated water. RNA was quantified using a NanoDrop Spectrophotometer ND-1000, and up to 5 µg of total RNA was used for cDNA synthesis. Following the manufacturer's instructions, cDNA was synthesized using the SuperScript® III First-Strand Synthesis System for RT-PCR (Invitrogen) with oligo-dT primers.

Semi-quantitative RT-PCR

For PCR we used 1 µl of cDNA diluted 1:5 and Crimson Taq™ DNA polymerase (New England Biolabs Inc.) was used according to manufacturer's protocol. The PCR conditions were as follows, 95˚C for 2 min; 25 cycles of 95˚C for 30 sec, 56˚C for 30 sec, and 72˚C for 30 sec; 72˚ for 5 min. PCR products were loaded on a 1.4 % agarose gel. PCR products ranged from 370 to 470 bp. As internal control we used primers (Table 4) to amplify a 448-bp DNA fragment from *Mtαtubulin* (GenBank

accession No. ES613496).

RNA blot analysis

Total RNA was extracted from leaves using TRI Reagent and dissolved in stabilized formamide. Total RNA was loaded on each lane and separated on 1 % agarose formaldehyde gel. Separated RNA was transferred (Sambrook et al., 2001) to Genescreen Plus nylon membrane (PerkinElmer, Boston, MA) and hybridized with radio-labeled probes (Church and Gilbert, 1984).

Methylglyoxal treatment

Eight healthy and fully expanded trifoliates were detached and weighed from A17, *cod*5 and *cod*6 plants. Trifoliates were floated in 0.1 % Silwet L-77 (Lehle seeds, Round Rock, TX), transferred to 1.5 mM methylglyoxal (MP Biomedicals LLC, Solon, OH) or water as a control and incubated for 84 h at 24°C with mild shaking. The treatment was carried out under continuous fluorescent white light. Chlorophyll was extracted and measured as described by Palta (1990).

Glyoxalase I activity assay

Glyoxalase I extraction was performed following the procedure described by Jain et al. (2002). Fresh leaf tissue taken from one fully expanded trifoliate was crushed with a mortar and pestle in 2 ml ice-cold 0.1 M sodium phosphate buffer (pH 7) containing 1 mM phenylmethylsulphonylfluoride (PMSF) and 10% (w/v) polyvinylpyrrolidone (PVP). Crude extract was transferred to a 1.5-ml Eppendorf tube and centrifuged for 10 min at 4°C at 10,000 x g. For chemical formation of the

hemithioacetal substrate, a solution containing 100 mM sodium phosphate buffer (pH 7.5), 3.5 mM MG, 1.7 mM reduced glutathione and 15 mM $MgSO_4$ $7H_2O$ was incubated for 7 min at 25°C in a final volume of 1 ml. Enzyme extract (25 µl) was added to the substrate solution, mixed by pipetting and absorbance was measured at 240 nm for 240 sec at 30 sec intervals using the Smart-Spec 3000 spectrophotometer (BIO-RAD). Protein concentration was determined using the Quick Start™ Bradford Protein Assay (BIO-RAD) following the manufacturer's instructions.

Production of constructs of glyoxalase I-like genes from *M. truncatula* to generate transgenic Arabidopsis plants

The open reading frames of TC122307 and TC122323 were amplified from cDNA using specific primers (Table 5) anchored with the BamHI and XbaI sites and cloned in the pCAMBIA2300s vector (modified from pCAMBIA2300, www.cambia.org) downstream the CaMV35S promoter (Fig. 15) and the presence of the each gene was confirmed by PCR and DNA sequencing. The individual constructs will be transformed into *Agrobacterium tumefaciens* strain GV3101.

Agrobacterium tumefaciens-mediated transformation will be performed based on the protocol developed by Clough and Bent (1998).

RESULTS AND DISCUSSION

Gene expression analysis of *cod* mutants via GeneChips

In an effort to compare gene expression profiles in *cod*5, *cod*6 and parental wild-type line A17, GeneChip® Medicago Genome Arrays (http://www.affymetrix.com) were probed with RNA taken from leaf tissue of the three genotypes (Korth, unpublished data).

The GeneChip® includes more than 50,000 *M. truncatula* probe sets. Hundreds of genes were found to be differentially regulated in the *cod* mutants using a *P*-value threshold of 0.05 and a log-ratio threshold of 0.1 (Fig. 2 and Fig. 4). The number of genes in the *cod* mutants with transcript levels varying significantly from those in A17 depends on the fold-change threshold used, with fewer genes identified using a lower *P*-value.

Using the set parameters, 193 genes are down-regulated in *cod*5 vs. A17 and 16 genes are down-regulated in *cod*6 vs. A17. Many fewer genes, only eight, were up-regulated in *cod*5 when comparing levels to expression in A17; and 20 genes were up-regulated in *cod*6. A considerable number of genes were differentially expressed in *cod*6 compared to *cod*5, 91 were up-regulated and 12 were down-regulated (Table 1).

Although *cod*5 and *cod*6 have a shared phenotype of greatly decreased concentrations of CaOX crystals in secondary veins (Nakata and McConn, 2000), there are substantial differences in overall gene expression between the *cod* mutants. When comparing both *cod* mutants with A17, only four genes are co-regulated in *cod*5 and *cod*6. All four were down-regulated and only functional category of two genes was

identified; one being involved in transcription regulation and the other gene annotated as a cytochrome P450. It is important to note here that although *cod*5 and *cod*6 both have severely decreased CaOX concentrations, *cod*6 will sometimes accumulate low levels of crystals in secondary veins and low levels of sand crystals in mesophyll cells, whereas CaOX is never visible in leaf tissue of *cod5* (Nakata and McConn, 2000).

The formation of CaOX crystals in plants is widespread among hundreds of plant families and the crystals can accumulate to very high levels. In spite of their abundance and these crystals being studied for many years, the physiological role(s) of CaOX in plants is still debated. One of the most common proposed roles for this mineral is the regulation and/or sequestration of excess calcium within cells (Libert and Franceschi, 1987). Calcium itself is a highly abundant element in plant cells, reaching concentrations of 30 to 90 nM in the cytoplasm and > 5 μM within the vacuole (Clarkson et al., 1988). Furthermore, calcium concentration is known to be a very important factor in gene regulation, physiological events, and enzyme activities in plants (Kim et al., 2009; Roberts and Harmon, 1992). Therefore, if the formation of CaOX in *M. truncatula* is necessary for fine-tuned regulation of calcium concentrations, then one might predict that the absence of crystals would lead to varied calcium levels which would result in a high number of genes being co-regulated in *cod*5 and *cod*6. We did not observe such co-regulation. Based on this result, we conclude that it is unlikely that CaOX formation plays an important role in regulating downstream gene expression profiles. These data would seem to be in agreement with a previous study from McConn and Nakata (2000). In a careful comparison of phenotypic *cod*5 and A17 plant performance in greenhouse and growth chamber studies, McConn and Nakata (2003)

concluded that CaOX formation was not important in regulating physiological outcomes. The only biological function that be assigned to CaOX crystals in *M. truncatula* thus far, is the deterrent and anti-nutritive activities that they have on chewing insects (Korth, et al., 2006).

Cluster analysis of GeneChip data shows similar expression patterns between *cod*6 and A17 in which most of the genes have higher expression levels (Fig. 2, cluster 4). The largest subset of differentially regulated genes showed lower expression levels in *cod*5 and are represented by clusters 3 and 4 (Fig. 2). In order to identify relevant biological functions associated to each probe set in the largest group, we used the GeneBins public database (http://bioinfoserver.rsbs.anu.edu.au/utils/GeneBins/) (Goffard and Weiller, 2007). The largest class of the down-regulated transcript sequences in *cod*5 corresponds to unclassified sequences making up 37 % of the total, followed by 10 % being genes involved in carbohydrate metabolism and 8 % in transcription regulation (Fig. 3). Other biological functions suggested to be down-regulated in *cod*5, each with 6 % of the total differentially expressed products, are signal transduction and glycan biosynthesis and metabolism. Five percent of the differentially expressed genes have no homolog. Three groups are each represented by 5 % of the genes; biodegradation of xenobiotics, metabolism of cofactors and vitamins, and cell growth/death. The functional categories of ligand-receptor interaction, amino acid metabolism, lipid metabolism, biosynthesis of secondary metabolites, energy metabolism, transport, cell communication and folding sorting and degradation are represented by one to three percent of genes (Fig. 3). Therefore, a single mutation affecting CaOX formation in *cod*5 likely causes an important change in gene expression

impacting many other processes in plant metabolism; however those changes do not affect plant performance (Nakata and McConn, 2003). Carbohydrate metabolism is the category represented by the highest number of down-regulated genes in *cod*5. This mechanism could potentially affect growth of CaOX crystals in *cod*5, as it was previously showed that polysaccharides are one of the factors that affect crystal growth and morphology (Kok et al., 1986). The second largest group of down-regulated genes with an ascribed function in *cod*5 is transcription regulation. The set of genes in this functional category could be also causing changes in expression of genes involved in other processes. There is a possibility that the mutation responsible for the CaOX phenotype in *cod*5 is not directly associated with CaOX formation and control transcription of genes involved in carbohydrate metabolism causing a reduction of CaOX formation to undetectable levels.

The difference in the CaOX phenotype between the *cod* mutants is that *cod*6 contains small crystals along the vascular strand and *cod*5 completely lack crystals (Nakata and McConn, 2000). Therefore, the relatively low presence of CaOX crystals in *cod*6 could be a result of the up-regulation of one or more genes. In *cod*6 we found 91 up-regulated genes as compared to expression in *cod*5 (Table 1). The lack of overlap in gene expression in the *cod* mutants also suggests that many genes affect crystal formation; this is in agreement with previous observations indicating that multiple genes control crystal formation in *M. truncatula* (Nakata and McConn, 2000). Again, it also suggests that expression of hardly any genes is impacted by a decrease in CaOX concentrations.

The *cod* mutants used in this study were generated from an EMS-mutagenized population and they have been backcrossed at least twice (Nakata and McConn, 2000). Even though the mutant lines have a single mutation with respect to CaOX phenotype, there is a possibility of these lines carrying mutations not associated with CaOX phenotype. The mutated genes in the *cod* mutants have not been yet identified; therefore differences of transcript profiles in the *cod* mutants could possibly be associated with other mutations.

Response of *M. truncatula cod* mutants to salt stress

Among the differentially expressed genes in A17, *cod*5 and *cod*6, we identified one annotated as encoding a putative glyoxalase I, also referred to a lactolylglutathione lyase. This gene has the distinction of being highly expressed in *cod*6 and severely down-regulated in *cod*5, as compared to constitutive expression levels in A17 (Fig. 4). This glyoxalase I-like gene, referred by its MtGI tentative consensus number TC122307, is expressed at levels 9.06-fold higher in *cod*6 compared to A17, and 11.6-fold lower in *cod*5 versus A17 (Table 2). This result was validated with RNA blot from leaf tissue of *cod* mutants and A17 (data not shown). Another glyoxalase I-like gene, TC123769, was 4.63 fold higher in *cod*6 as compared to A17 (Table 2) and 19.13 fold higher in *cod*6 as compared to *cod*5. The glyoxalase I-like predicted mRNA sequences were aligned to each other and have a 79.9 % identity at the nucleic acid level. The expression pattern for these genes in the *cod* mutants was rare among our array data, in that transcript accumulation was significantly different from A17, and was inverse in the two *cod* mutants.

Transcripts and polypeptide levels of GLXI increase in tomato roots, stems and leaves from plants treated with NaCl, mannitol or abscisic acid (Espartero et al., 1995). Furthermore, overexpression of *GLXI* from *Brassica juncea* was previously shown to increase tolerance to NaCl in transgenic tobacco plants (Veena et al., 1999). Therefore, the increase in salt tolerance by overexpressing this gene shows that GLXI plays a role in salt tolerance. Because glyoxalase I-like genes were up-regulated in *cod*6 and down-regulated in *cod*5, we surmised that this plant system would provide a valuable resource for evaluating the potential role of this enzyme in conferring salt tolerance in *M. truncatula*. We evaluated tolerance to salt stress in the *cod* mutants to determine whether this putative GLXI was associated with salt tolerance to *cod*6.

Increasing concentration of NaCl caused appearance of associated salt stress symptoms in the three genotypes after four weeks of treatment as reflected by phenotypic rating. Although *cod*6 showed substantial growth inhibition as compared to water-treated controls, this genotype showed considerably less necrosis and chlorosis as compared to *cod*5 and A17. On the other hand, *cod*5 showed more leaf chlorosis and necrosis, while A17 showed less salt-stress symptoms than *cod*5 (Fig. 5). The three genotypes did not show any symptoms following application of 50 mM $CaCl_2$, or water (Fig. 5). In general, *M. truncatula* genotypes were more sensitive to sodium than calcium salt, as shown by the response to NaCl treatments. This is a common response in glycophytes (Bernstein and Hayward, 1958), and further suggests that in this case much of the damage to the plant results from the sodium cation rather than the chloride anion. Phenotypic rating was performed to evaluate salt tolerance. Our results showed that *cod*6 had significantly less symptoms compared to *cod*5 and A17 ($P < 0.001$) (Fig.

6B). In addition, chlorophyll content (Fig. 6C) and fresh weight (Fig. 6D) were significantly higher in *cod*6 after the NaCl treatment confirming the results from the phenotypic rating. In contrast, A17 and *cod*5 had similar responses to NaCl treatment as shown by phenotypic rating, chlorophyll content and fresh weight (Fig. 6). Together these results provide evidence for tolerance to salt stress in *cod*6, suggesting the high level of expression of the genes encoding TC122307 and TC123769 is associated with this trait.

Under salt stress conditions in rice cell cultures, glycolysis and TCA cycle enzymes are induced (Umeda et al., 1994) which may increase the production of MG, a by-product of glycolysis. Subsequently, activity of the enzymes of the glyoxalase system may increase as well (Espartero et al., 1995). Therefore, plants respond to salt stress by enhancing rates of glycolysis and ultimately increasing activity of the glyoxalase system to detoxify MG. This could be a good explanation for salt tolerance by the up-regulation of *GLXI*.

Mineral analysis of salt-treated plants

We measured calcium, sodium, and chloride levels from foliar tissues of NaCl-, $CaCl_2$- and water-treated plants. Our results show similar sodium levels in the three genotypes following salt treatments, which indicate that all the lines are uptaking sodium. However, as we discussed above *cod*6 show less symptoms under high salinity conditions, therefore *cod*6 has mechanisms to cope with these conditions when compared to *cod*5 and A17. Chloride levels were also similar in the three genotypes even when NaCl or $CaCl_2$ was applied, indicating that all the lines have the ability to

uptake chloride, however they do not seem to exclude chloride. In many other plant species, such as *Glycine*, *Lotus*, *Hordeum*/*Triticum*, *Trifolium* and *Eucalyptus* chloride exclusion from shoots correlate with salt tolerance (Teakle and Tyerman, 2010). In *M. truncatula* it has been suggested that both sodium and chloride exclusion contribute to salt tolerance (Aydi et al., 2008). Our results show that the *cod* mutants and wild-type A17 take up sodium and chloride in similar levels (data not shown). In the case of sodium, none of the lines seem to exclude sodium either, but *cod*6 has a mechanism to cope with high sodium levels as reflected by salt treatments (Fig. 5, 6).

In a previous study, Nakata and McConn (2003) found similar calcium levels in leaves of *cod*5 and A17 under normal conditions. In addition, this study measured oxalate content in leaf tissue and based on comparison of calcium and oxalate content in *cod*5 and A17, concluded that crystal formation is not necessary to sequester excess calcium in *M. truncatula*. In other plant species it has been shown that CaOX crystals play a major role in calcium regulation by sequestering excess calcium (Nakata, 2003).

We measured calcium in leaves of salt-treated plants; sodium chloride and water applications resulted in similar calcium levels in *cod* mutants and A17. The addition of $CaCl_2$ to *cod* lines caused a significant increase (t-test, $P < 0.05$) in calcium content of *cod*5 compared to wild-type A17 (Fig. 7). Such increase was also higher in *cod*6 compared to A17 although the difference was not significant (t-test, $P > 0.05$). These results may suggest that the lack of mechanisms to sequester calcium as CaOX crystals leads to the higher calcium content in leaves of *cod*5 suggesting that CaOX crystal formation plays a role in sequestering excess calcium in *M. truncatula*. However, more research will be needed to confirm this statement.

Calcium concentration in the cells is restricted in plants to ~10^{-7} M in order to prevent a negative impact of this element to distinct cellular processes (Webb, 1999). Many studies proposed that plants produce CaOX crystals in response to higher levels of calcium (Franceschi and Horner, 1980; Franceschi and Nakata, 2005). In this respect, the vacuole has been recognized as the most important organelle for compartmentation of excess calcium (Webb, 1999; Ilarslan et al., 2001). It is also possible that one or more down-regulated genes in *cod*5 are involved in calcium transport via the activity of channels or pumps (Franceschi and Nakata, 2005) to the vacuoles consequently lacking mechanisms to form CaOX crystals. In this respect, in the GeneChip array data we found a gene (GenBank: AY059633.1) encoding a putative *M. truncatula* type IIB calcium ATPase (*MtMCA2*) which is 3.88 fold lower in *cod*5 as compared to wild-type.

Type IIB Ca^{2+}-ATPases from higher plants have been localized to endomembranes (Geisler et al., 2000) and the main role of Ca^{2+}-ATPases localized in the plasma membrane and endoplasmic reticulum (ER) is the regulation of Ca^{2+} concentration in the cytoplasm (Briskin, 1990; Bush, 1995). In tomato, a Ca^{2+}-ATPase expected to be localized in the ER was found to be induced by salt stress (Wimmers et al., 1992). Even in the moss, *Physcomitrella patens*, transcripts from a Ca^{2+}-ATPase (*PCA1*) accumulate in higher levels by dehydration, NaCl and abscisic acid (Qudeimat et al., 2008). Moreover, mutants lacking a functional *PCA1* showed higher susceptibility to salinity stress, indicating that Ca^{2+}-ATPase is essential for stress tolerance in the moss (Qudeimat et al., 2008).

The function of Ca^{2+} in stress tolerance has not been defined yet; however the rapid increase in cytosolic Ca^{2+} levels during salt stress suggests that Ca^{2+} probably functions as a stress signal (Niu et al., 1995). Therefore, it has been previously proposed that the increase in cytosolic Ca^{2+} during salt stress could be potentially decreased by the enhanced activity of Ca^{2+}-ATPase (Niu et al., 1995). In the case of *cod*5, a putative Ca^{2+}-ATPase is down-regulated and therefore it could contribute to more sensitivity to salt stress in this *cod* mutant.

Glyoxalase I activity in the *cod* mutants

In *Brassica juncea*, transcript levels of a gene encoding GLXI correlated with protein and GLXI activity levels from cotyledonary leaves and roots (Veena et al., 1999). We measured GLXI activity from *cod* mutants and A17 to determine whether TC122307 and TC123769 transcript levels correlate with GLXI enzyme activity. If these genes encode GLXI, we would expect higher levels of GLXI activity in *cod*6 and decreased levels in *cod*5, compared to enzyme activity in A17. However, enzyme assays show that GLXI activity in leaf tissue from A17 and the *cod* mutants is not significantly different (Fig. 8). These results were similar in three independent measurements, suggesting that TC122307 and TC123769 do not encode GLXI.

Tolerance to Methylglyoxal

Methylglyoxal is the substrate of GLXI (Thornalley, 1990), therefore plants producing high levels of GLXI have the ability to detoxify MG and prevent its toxic effect. Previous studies showed MG tolerance in transgenic lines overexpressing *GLXI*

by measuring chlorophyll content from MG -treated leaves (Veena et al., 1999; Singla-Pareek et al., 2003). We analyzed MG tolerance in leaves from *cod* mutants to determine whether overexpression of TC122307 and TC123769 in *cod*6 would confer tolerance to MG. Chlorophyll contents from *cod* mutants and A17 were very similar in untreated leaves, however following an 84-hour MG treatment chlorophyll content decreased significantly in each of the genotypes (Fig. 9). The *cod* mutants were equally sensitive to the treatment. We did not observe enhanced tolerance to MG in *cod*6; therefore TC122307 and TC123769 are not likely to encode GLXI, confirming enzyme activity data from leaves which also suggested that these genes do not encode GLXI.

Sequence analysis of glyoxalase I-like genes

In a search of the *M truncatula* EST database, we identified a glyoxalase I-like gene (TC122323) 90.3 % identical to glyoxalase I from *Glycine max* (GmGlxI). Predicted amino acid sequences from genes annotated as glyoxalase I in *M. truncatula* were aligned with GLXI proteins confirmed as having GLXI enzyme activity. Multiple sequence alignment shows conserved amino acids that form the zinc binding sites shared by TC122323 and other characterized GLXI sequences (Fig. 10). In addition, the predicted secondary structure (βαβββ) characteristic of the VOC superfamily (Armstrong, 2000) is shared by TC122323 and characterized GLXI proteins. The gene sequences of TC122307 and TC123769 are not predicted to encode the conserved amino acids that form the zinc-binding domain which is essential for GLXI activity (Mannervik and Ridderstrom, 1993). These genes are, however, predicted to encode the βαβββ structure as predicted by PSIPRED (Bryson et al., 2005) (data not shown).

Taken together, our data strongly suggest that TC122307 and TC123769 are misannotated as GLXI, but are members of the VOC superfamily. This sort of result is supported in a study by Schnoes et al. (2009), which showed a gene misannotated as *GLXI* but found to encode a glutathione transferase. The explanation for this misannotation is that families within a superfamily share tertiary structure (one or more βαββββ), but catalyze distinct reactions which make the annotation process more complex (Schnoes et al., 2009).

A phylogenetic tree was generated to visualize the genetic relationship between the three genes identified as members of the GLXI family in *M. truncatula* (Fig. 11). As we expected, TC122307 and TC123769 do not appear to be GLXI proteins. However, TC122307 and TC123769 are grouped closer to novel members of the VOC superfamily (Mulako et al., 2008). These novel members include *Xhdsi-1*^{VOC} from *Xeropjhyta humilis* and *At1g07645* from Arabidopsis which are induced during dessication (Mulako et al., 2008); therefore it is interesting to note that TC122307 and TC123769 as members of the VOC superfamily also play a role in abiotic stress. In addition, TC122323 groups closer to GmGlxI and other characterized glyoxalase I, suggesting that TC122323 encodes the authentic GLXI in *M. truncatula*.

Gene expression analysis of *GLXI*-like genes following salt treatments

We analyzed gene expression of *GLXI*-like genes TC122307, TC123769 and TC122323 in *M. truncatula* following NaCl and water applications at three days and one week after initial application. Transcripts of TC122307 accumulate in A17 and *cod*6 after three days of initial application of NaCl (Fig. 12). Higher transcript levels

were detected in *cod*6 as compared to constitutive expression in A17. We did not detect transcripts of TC122307 in *cod*5 after NaCl. Comparing these results with water-controls we conclude that NaCl does not induce transcript accumulation in TC122307 in any of the lines. After one week of initial salt-treatments we did not observe changes in expression of TC122307 compared to expression levels after three days. Same expression pattern was observed for TC123769 after three and one week of initial treatment in all the lines. This could be due to the fact that both genes are almost 80 % identical at the nucleic acid level. Together, these results suggest that TC122307 and TC123769 are co-regulated. Based on gene expression analysis both genes are possibly controlled by similar transcription factors; therefore we aligned sequences from the upstream regions of T122307 and TC123769 but did not find similarity (data not shown). On the other hand, transcript abundance of TC122323 was uniform in the three genotypes under all conditions, showing that it is constitutively expressed in the *cod* mutants and A17.

Transcript abundance of glyoxalase I-like genes in *M. truncatula* was also evaluated using a semi-quantitative RT-PCR approach to exclude the possibility that co-regulation of TC122307 and TC123769 in the RNA blot data (Fig. 12) was caused by cross hybridization (Fig. 13). Gene-specific primers were designed to amplify a 370 to 470 fragment from the ORF of each gene (Table 4). Our results agree with the RNA blot data in that TC122307 and TC123769 are co-regulated and TC122323 is uniformly expressed in the three genotypes under normal conditions. Even though many reports show an increase of *GLXI* transcripts and GLXI activity following salt treatments (Espartero et al., 1995; Veena, 1999, Lin et al., 2010) and assuming that TC122323 is

the authentic *GLXI*, this gene is not induced by salinity stress in *M. truncatula*. A similar response has been reported where GLXI activity had no change after salt treatment in tobacco cells (Hoque et al., 2008). These results suggest that the up-regulation of glyoxalase I is not a general effect against abiotic stresses.

We also analyzed gene expression of TC122307 following $CaCl_2$ in leaf tissue from *M. truncatula* to evaluate if transcript abundance was affected by this salt (Fig. 14). We conclude that $CaCl_2$ does not have an effect on transcript accumulation of TC122307, because we did not observe any change in mRNA levels in *cod* mutants and A17 compared to water control.

Production of transgene constructs of *GLXI*-like genes from *M. truncatula*

We generated constructs to overexpress TC122307 and TC122323 in Arabidopsis. The open reading frames of TC122307 and TC122323 were independently amplified by PCR from cDNA using primers (Table 5) containing restriction sites (Fig. 16). We cloned the genes into pCAMBIA2300s vector containing a CaMV 35S promoter upstream the ORF from TC122307 or TC122323 (Fig. 15, 17). The integrity of the genes was confirmed by restriction digestion (Fig. 18), PCR (Fig. 19), and sequencing (data not shown). Transgenic plants will be produced by inoculating Arabidopsis plants with *A. tumefaciens* carrying a pCAMBIA2300s containing TC122307 or TC122323 using the floral dip method (Clough and Bent, 1998). These plants will be used to assess the role of these genes in salt adaptation by evaluating their performance under high salt conditions.

CONCLUSIONS

Gene expression data of *M. truncatula cod* mutants obtained with GeneChip arrays show major differences in transcriptomes of *cod*5, *cod*6, and wild-type A17. Hundreds of genes were found to be differentially expressed when the *cod* mutants were compared to each other, although the mutants share a very similar phenotype with respect to CaOX crystals. Therefore, we conclude that CaOX formation is not likely to impact calcium modulation that would ultimately regulate gene expression patterns.

In the array data we identified two *GLXI*-like transcripts (TC122307 and TC123769) overexpressed in *cod*6 and down-regulated *cod*5. Because previous studies show that up-regulation of *GLXI* in transgenic plants confers resistance to salt stress (Veena et al., 1999; Singla-Pareek et al., 2003), we analyzed the response of *cod* mutants to salinity. Salt treatments showed that *cod*6 is more tolerant to NaCl stress compared to wild-type A17, and *cod*5, the latter being the most sensitive. We found a connection between expression profiles of these *GLXI*-like genes and salt tolerance in the *cod* mutants. However, mRNA levels of TC122307 and TC123769 do not increase following salt application as shown in other characterized *GLXI* genes (Veena et al., 1999; Espartero et al., 1995; Lin et al., 2010). Enzymatic GLXI activity was similar in the *cod* mutants and A17. In addition, all the lines were equally sensitive to toxic levels of methylglyoxal, the substrate of GLXI. These results show that it is highly probable that TC122307 and TC123769, both annotated as *GLXI*, do not encode functional GLXI. This conclusion is further supported by the predicted amino acid sequences encoded by these two transcripts. Based on multiple sequence alignment, these genes

are members of the VOC enzyme superfamily but they do not contain the hallmark metal-binding sites associated with authentic GLXI enzymes.

Gene expression analyses showed that TC122307 and TC123769 are not induced by salt stress and that both genes are co-regulated. Another gene, encoding TC122323, is predicted to be translated to a putative GLXI; however, this gene is not induced by salt stress either. We found that TC122323 is constitutively expressed in the *cod* mutants and A17; which probably explains the similar responses of all genotypes to methylglyoxal and the similar levels of GLXI activity in leaf tissue. These results and sequence analysis indicate that TC122323 is the authentic *GLXI* in *M. truncatula*, although functional characterization of enzyme activity has not been demonstrated.

In conclusion, the *cod6* mutant which expresses high levels of transcripts for two predicted members of the VOC superfamily displays considerably enhanced levels of salt tolerance. Although the specific substrate(s) of the encoded proteins is unknown, the underlying genes represent excellent candidates for further study and engineering of increased salt tolerance in plants.

Figure 1. Steps in the conversion of methylglyoxal to D-lactic acid by the glyoxalase system. A non-enzymatic reaction generates the hemithioacetal from methylglyoxal and reduced glutathione (GSH); the hemithioacetal is in turn converted to *S*-D-lactoylglutathione by glyoxalase I (GLXI). Another enzyme, glyoxalase II (GLXII), catalyzes the hydrolysis of *S*-D-lactoylglutathione to D-lactic acid with the regeneration of GSH.

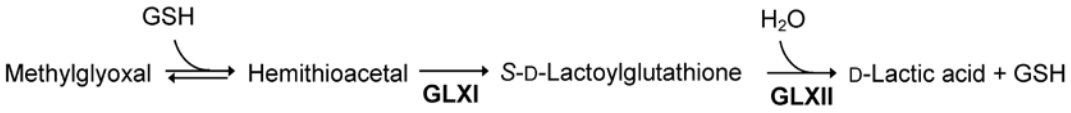

Figure 2. Heat map showing a graphical representation of average probe intensity for each plant genotype. Intensities of each probe are comparisons of *cod*5 versus A17 and *cod*6 versus A17 and the colors represent these relative levels. Higher expression is represented by red, lower expression by green, white indicates no value and black is mid-range between high and low expression. Probes were split into five clusters to illustrate the expression patterns between the three genotypes. The largest clusters (3 and 4) assemble the largest subset of differentially expressed genes.

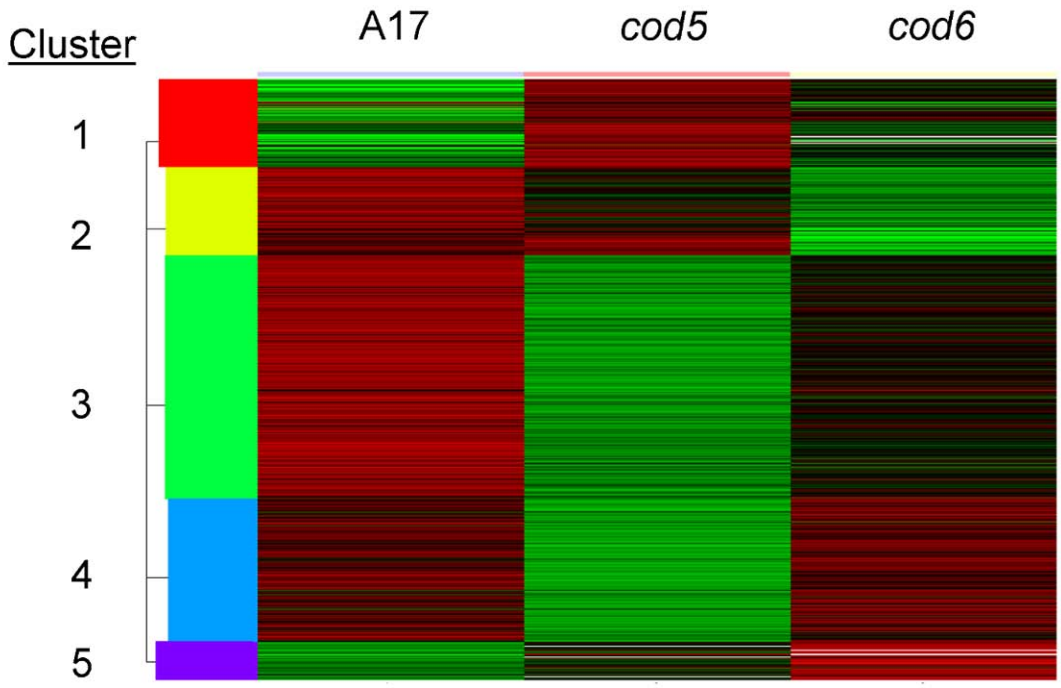

Table 1. Number of genes differentially expressed in the *cod* mutants with respect to expression in A17.

	***cod5* vs. A17**	***cod6* vs. A17**	***cod6* vs. *cod5***
Up-regulated	8	20	91
Down-regulated	193	16	12

Figure 3. Functional categories of down-regulated genes in *cod*5. GeneBins was used to classify gene expression data. The majority of the classified genes are in the carbohydrate metabolism category.

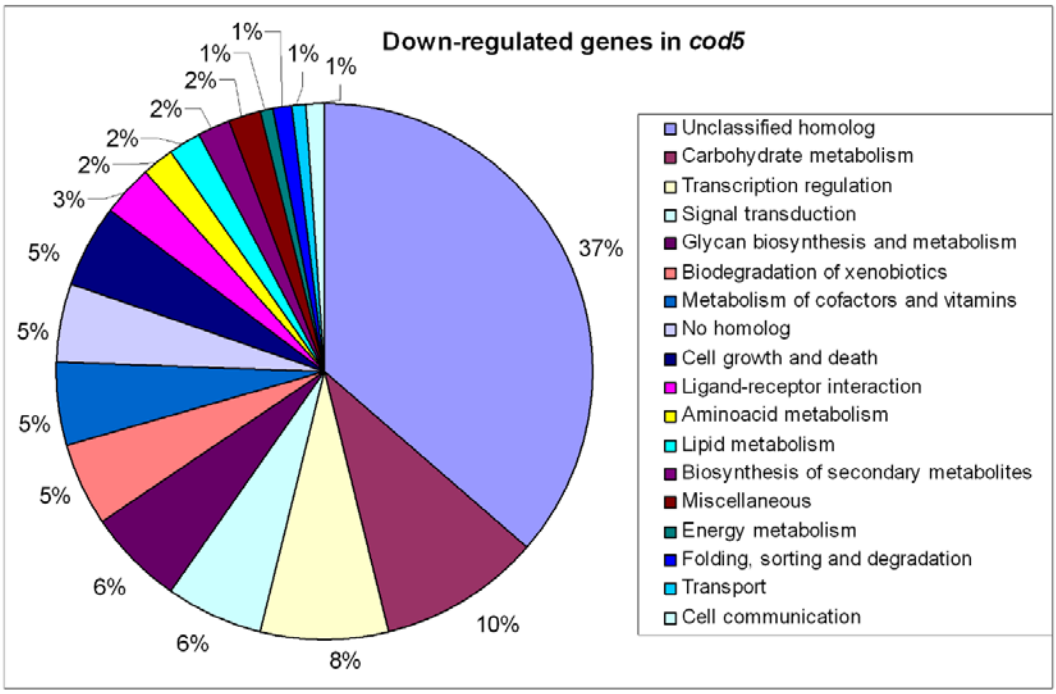

Figure 4. Heat map highlighting expression pattern of a subset of genes in cluster 1 (as shown in Figure 1), grouped with TC122307. Intensities of each probe are compared in A17 vs. *cod*5 and A17 vs. *cod*6, and the colors represent these relative levels. Higher expression is represented by red, lower expression by green, white indicates no value and black is midrange between high and low expression.

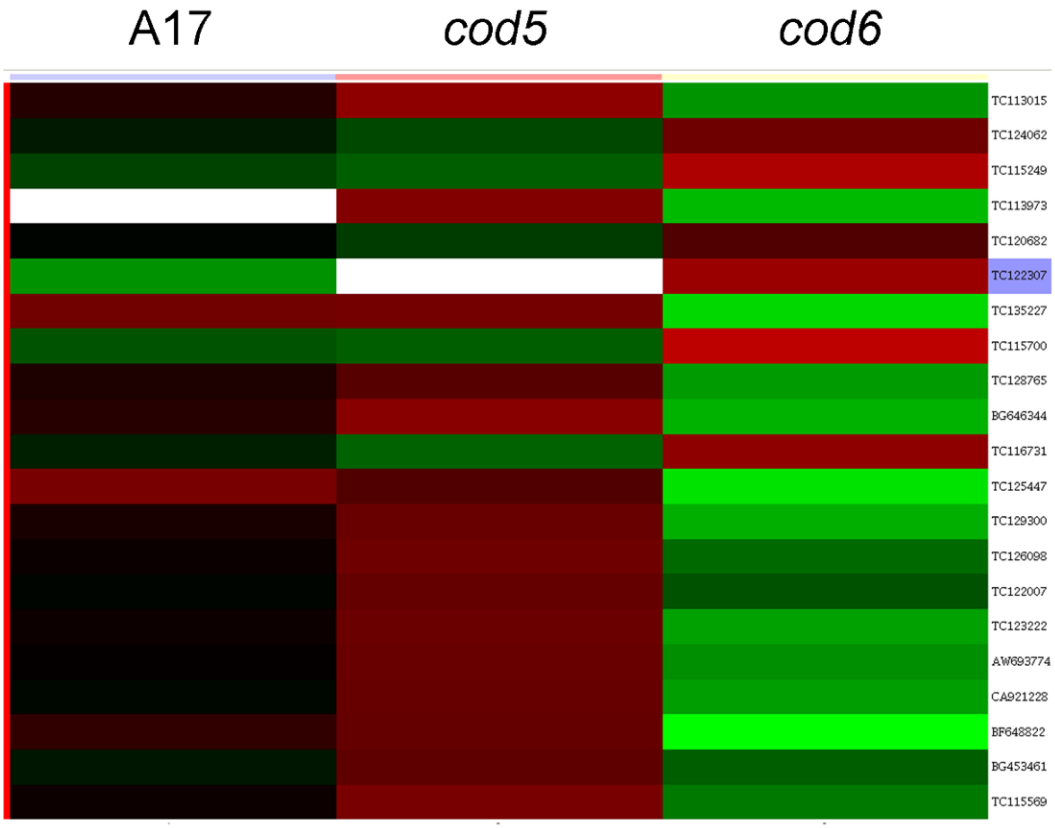

Table 2. List of up-regulated genes in *cod*6 compared to A17. The number of unclassified genes is 14, and 10 genes do not have a significant match in the Genbank database.

TC No. or public ID	Tentative annotation	Fold change	Blastx E-value	Biological process
TC98216	Chalcone reductase	2.02	1.00E-31	Flavonoid biosynthesis
TC94733	triacylglycerol lipase	2.3	2.00E-30	Lipid metabolism
IMGAG|890.m00012	UDP-glucosyltransferase	2.4	3.00E-142	Biosynthesis of secondary metabolites
BI265018	Ca2+:H+ antiporter	2.91	5.00E-41	Membrane transport
TC104995	Squamosa promoter binding protein-like 8	3.01	6.00E-40	Transcription regulation
BI272694	Tetracycline transporter protein-like	3.03	6.00E-44	Membrane transport
BF637445	Ca2+/H+ exchanger	3.68	4.00E-09	Membrane transport
TC123769	lactoylglutathione lyase	4.63	4.00E-41	Carbohydrate metabolism
TC122307	lactoylglutathione lyase	9.06	2.00E-45	Carbohydrate metabolism

Table 3. List of down-regulated genes in *cod*6 compared to A17. The number of unclassified genes is seven, and five did not have a significant match in the Genbank database.

TC No. or public ID	Tentative annotation	Fold change	Blastx E-value	Biological process
IMGAG|816.m00029	Cytochrome P450	-2.81	1.00E-158	Carbohydrate metabolism, biosynthesis of secondary metabolites, biodegradation of xenobiotics, lipid metabolism, aminoacid metabolism
TC102088	Cytochrome P450	-2.63	8.00E-100	Carbohydrate metabolism, biosynthesis of secondary metabolites, biodegradation of xenobiotics, lipid metabolism, aminoacid metabolism
TC95921	Dehydration-responsive element-binding protein 1B (DREB1B protein)	-2.19	1.00E-14	Transcription regulation
IMGAG|797.m00001	Aldo/keto reductase	-2	2.00E-56	Carbohydrate metabolism, biodegradation of xenobiotics, lipid metabolism

Figure 5. Response of *M. truncatula cod* mutants to salt stress. Plants showing symptoms following treatment with 100 mM NaCl, 50 mM $CaCl_2$, or water (H_2O) for four weeks.

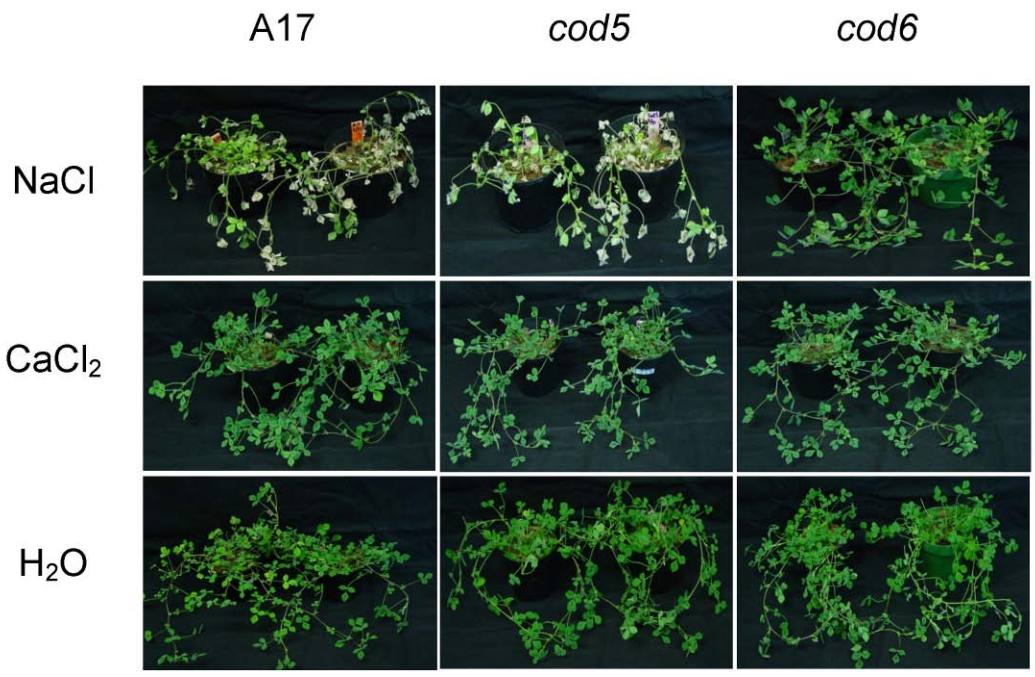

Figure 6. Effect of salinity stress in the *cod* mutants. Plants were treated with 100 mM NaCl or water (H_2O). (A) Phenotypic rating scale of 1-6, 1 for healthy plant with no chlorosis and 6 for complete leaf necrosis and plant death (B) Phenotypic rating, (C) Chlorophyll content, and (D) Fresh weight were measured to evaluate tolerance to salt stress. Columns labeled with a star are significantly different (t-test, $P < 0.001$) within genotypes. The error bars indicate standard error.

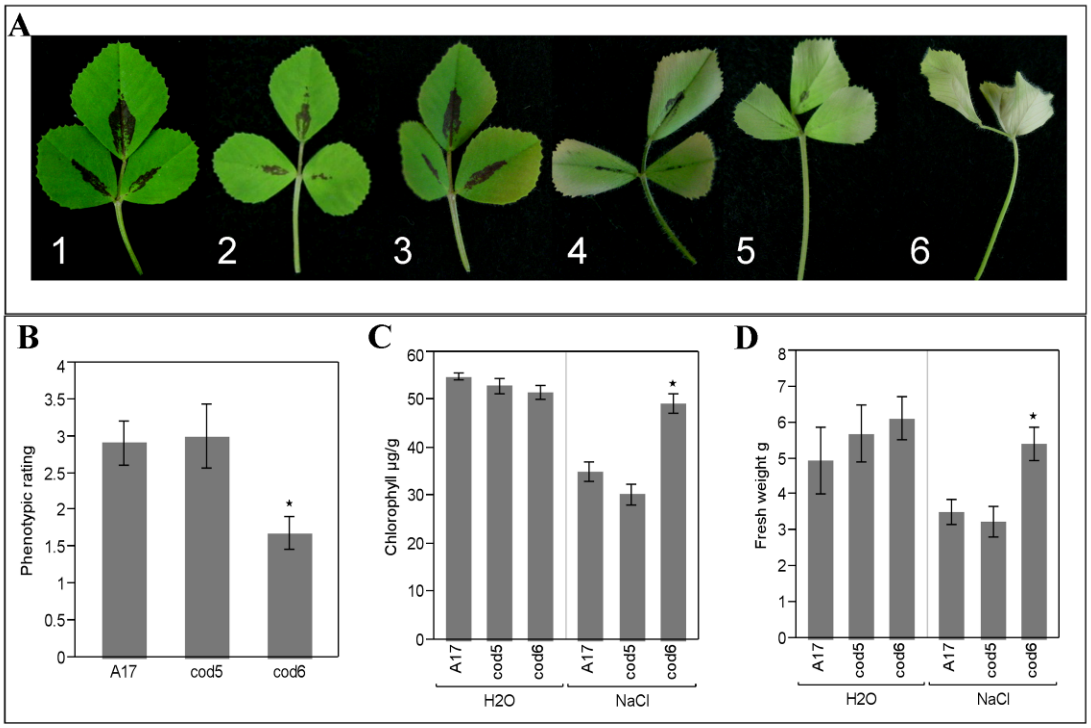

Figure 7. Calcium content in leaves of *cod* mutants following salt treatment. Plants were treated with 100 mM NaCl, 50 mM $CaCl_2$ or water (H_2O) for 4 weeks and dry tissue from leaves was used for calcium content measurement. Levels not connected by same letter are significantly different (t-test, $P < 0.05$). The error bars indicate standard error.

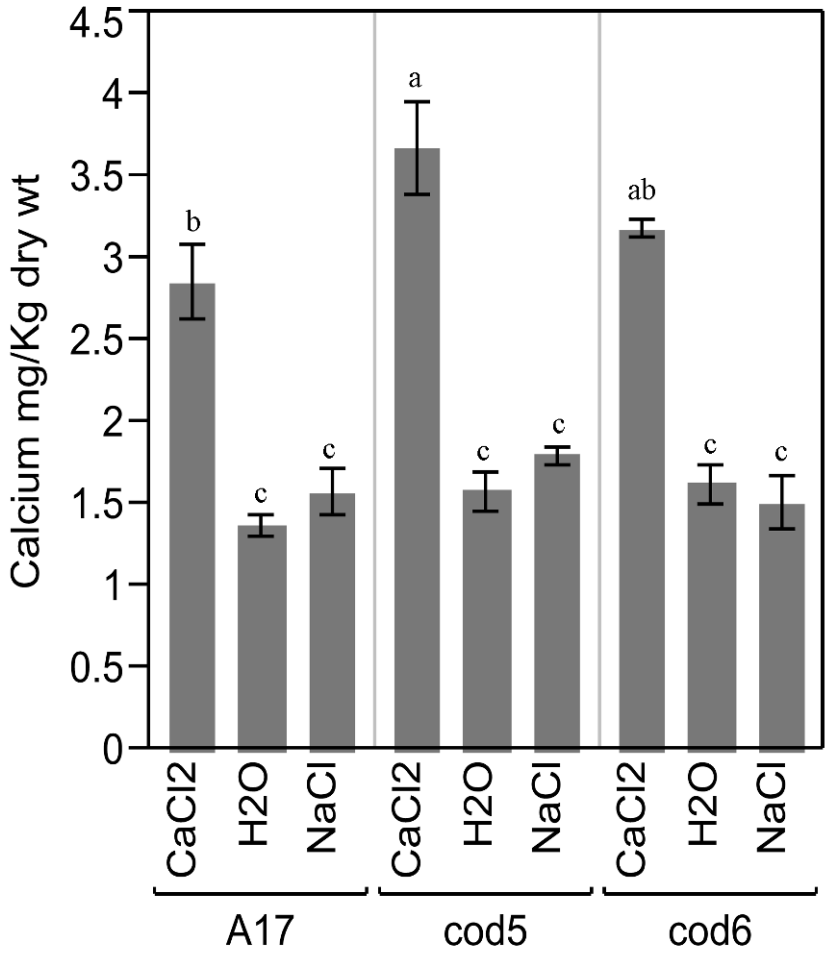

Figure 8. Glyoxalase I activity in leaf tissue of A17, *cod*5 and *cod*6. Graph represents data from one independent assay. One trifoliate from each genotype was collected for the assay. A unit is defined as the amount of enzyme that catalyzes the formation of 1 µmol of substrate per minute (NC-IUB, 1979). No significant difference was found between genotypes (t-test, $P > 0.05$). The error bars indicate standard error.

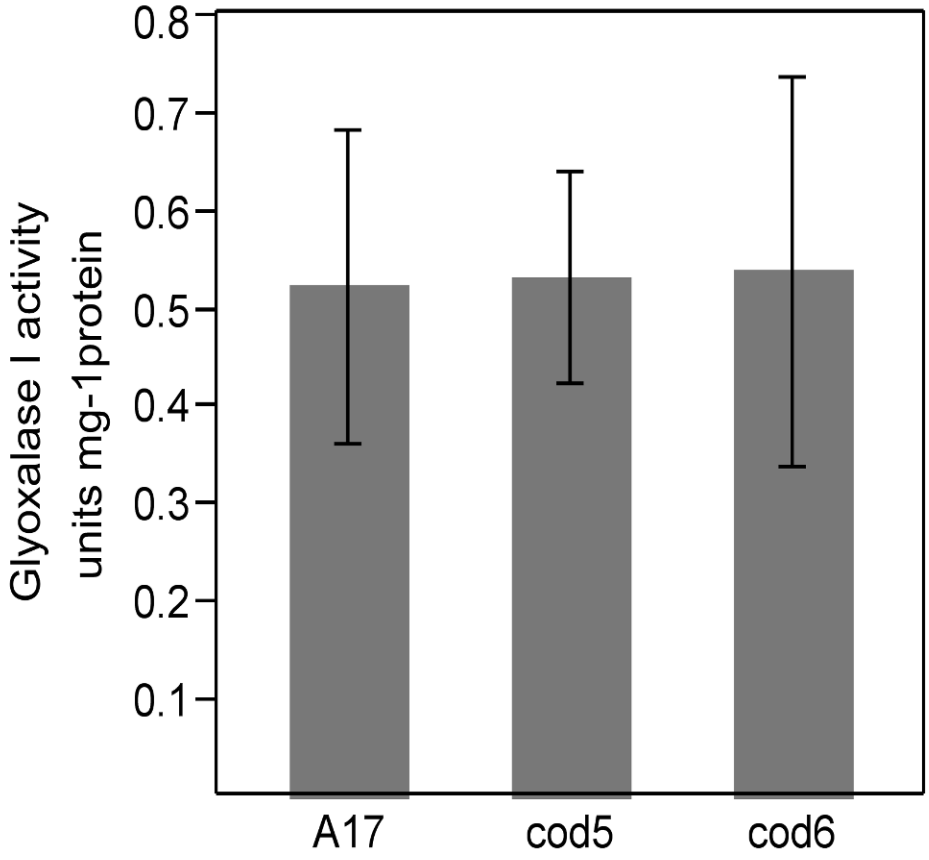

Figure 9. Methylglyoxal tolerance in the *cod* mutants. Chlorophyll content in *cod*5, *cod*6, and A17 was measured following 84 h incubation in 1.5 mM methylglyoxal to evaluate tolerance. Significant difference was found between treated and non-treated leaves (t-test, $P < 0.05$). The error bars indicate standard error

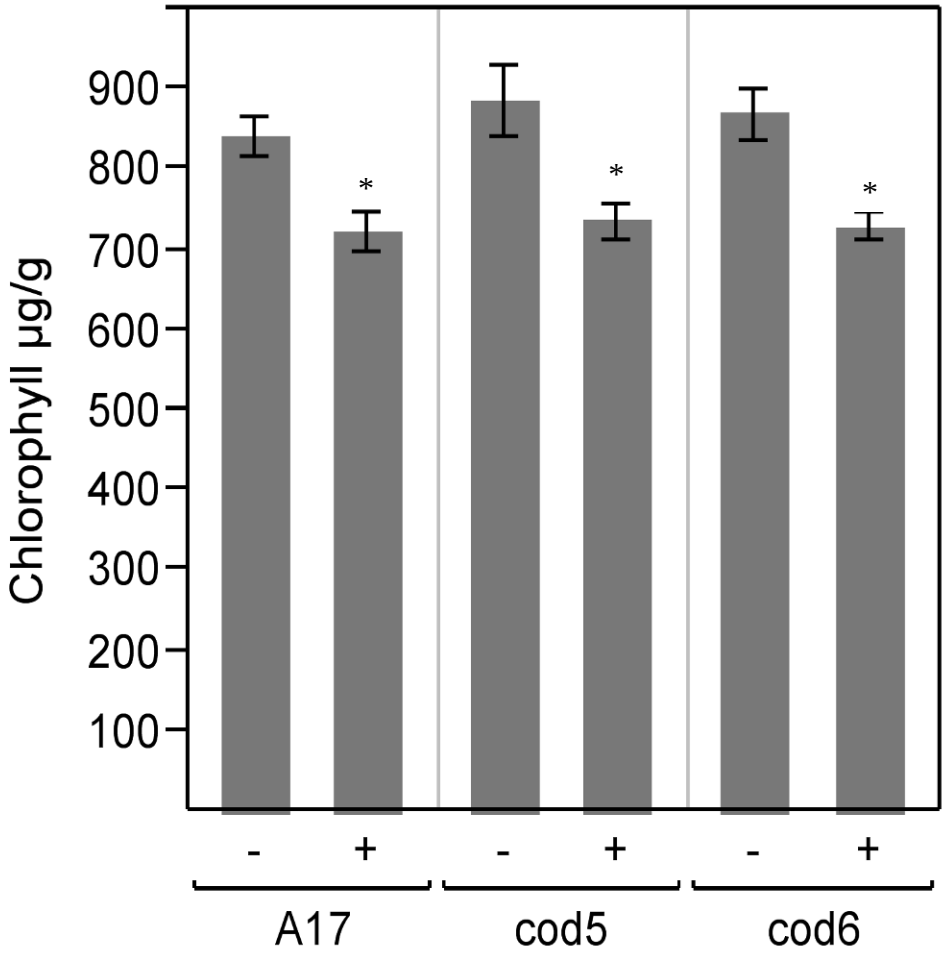

Figure 10. Multiple sequence alignment of deduced amino acid sequences of glyoxalase I-like genes in *M. truncatula* and previously reported glyoxalase I proteins from other plant species: *Glycine max*, GmGlxI (CAA09177.1), *Brassica juncea*, BjGlxI, (CAA73691), *Solanum lycopersicum*, SlGlxI (CAA88233), *Homo sapiens*, HsGlxI (AAD38008), TC122307, TC123769, TC122323. Conserved amino acids that form the zinc-binding sites are boxed. ClustalW program was used for the alignment. The asterisks (*) indicate conserved residues, two dots (:) indicate conserved substitutions, and one dot (.) indicates semi-conserved substitutions. Predicted secondary structure (βαββββ) characteristic of the VOC superfamily is indicated.

```
CLUSTAL W (1.81) multiple sequence alignment

                                                                  β1          α1
TC122323      ----MAASESKESP--ANNPGLHAT--VDEATKGYFMQQTMFRIKDPK----VSLDFYSR
GmGlxI        -----MAAEPKESP--SNNPGLHTT--PDEATKGYIMQQTMFRIKDPK----VSLDFYSR
SlGlxI        -----MASESKDSP--SNNPGLHAT--PDEATKGYFLQQTMFRIKDPK----VSLEFYSK
BjGlxI        -----MASEAKESP--ANNPGLSTV--RDEATKGYIMQQTMFRVKDPK----ASLDFYSR
HsGlxI        -----MAEPQPPSGGLTDEAALSCCSDADPSTKDFLLQQTMLRVKDPK----KSLDFYTR
TC123769      MEIEEVCEAQA-LPLLSLNHVSLLCRSVLESMQFYEDVLGFVPIKRPSSFKFTGAWFYNY
TC122307      MGIQEIGSYEAPLPLLSLNHVSILCRSVLDSMRFYEEILGFGLIKRPSSFKFNGAWLYNY
                          : :           : : :     :  :* *.      .  :*.

                  β2          β3                                  β4
TC122323      VLGMSLLKRLDFPEMKFSLYFMG-YEDTSEAPSNSVDRTVWTFAQKATIELTHNWGTESD
GmGlxI        VLGMSLLKRLDFPEMKFSLYFMG-YENTAEAPSNPIDKVVWTFSQKATIELTHNWGTESD
SlGlxI        VLGMSLLKRLDFPEMKFSLYFMG-YEDTASAPSDPVERTAWTFSQKSTLELTHNWGTESD
BjGlxI        VLGMSLLKRLDFSEMKFSLYFLG-YEDTSTAPTDPTERTVWTFGRPATIELTHNWGTESD
HsGlxI        VLGMTLIQKCDFPIMKFSLYFLA-YEDKNDIPKEKDEKIAWALSRKATLELTHNWGTEDD
TC123769      GIGIHLIQNPDIDEFDTYMNESRPINPKDNHISFQCTDVELVKKRLEEKGMRYVTALVED
TC122307      GFGIHLLENPNYDEFDTPMSESRPINPKDNHISFQCTDVGLVKMRLEDMGMKYVTALVED
               :*: *::. :   :.  :      : .    .       .  :     : :  .  .*
                                          β5          α2        β6          β7
TC122323      PEFKGYHNGNSDPRG-----FGHIGITVDDTYKACERFQNLGVEFVKKPEDGKMKGIAFI
GmGlxI        PEFKGYHNGNSEPRG-----FGHIGVTVDDTYKACERFQNLGVEFVKKPEDGKMKGIAFI
SlGlxI        PNFTGYHNGNSEPRG-----FGHIGVTVDDVYKACERFESLGVEFVKKPLDGKMKGIAFI
BjGlxI        PEFKGYHNGNSEPRG-----FGHIGVTVDDVHKACERFEQLGVEFVKKPHDGKMKNIAFI
HsGlxI        -ETQSYHNGNSDPRG-----FGHIGIAVPDVYSACKRFEELGVKFVKKPDDGKMKGLAFI
TC123769      EGIKVDQVFFHDPDGYMIELCNCENIPIIPISSCTASFKPRSHSFKRSTSNFKCG--GFM
TC122307      EGIKVEQVFFHDPDGYMIELCNCENIPIVPISSASGSFKARGQSFKKTVSN-KCG---FM
                    :    :* *      .  .:.:    ..   *:  . .* :.  : *     *:
                  β8
TC122323      KDPDGYWIEIFDRKTIGNVTGSAA
GmGlxI        KDPDGYWIEIFDRKTIGNVTQTAA
SlGlxI        KDPDGYWIEIFDTKIIKDAAGSAS
BjGlxI        KDPDGYWIEIFDLKTIGTTAGNAA
HsGlxI        QDPDGYWIEILNPNKMATLM----
TC123769      QN---VMMQSLSMDMMNFAF----
TC122307      EN---VMMRSLSKDMMNFAF----
              ::     :. :. . :
```

Figure 11. Phylogenetic tree of predicted *M. truncatula* glyoxalase I-like protein sequences (TC122307, TC123769, TC122323), previously characterized glyoxalase I (*Glycine max*, GmGlxI; *Brassica juncea*, BjGlxI; *Solanum lycopersicum*, SlGlxI; *Homo sapiens*, HsGlxI) and novel enzymes of the VOC superfamily (*Xerophyta humilis*, Xhdsi-1^{VOC}; *Arabidopsis thaliana*, At1g07645). Tree was generated via the neighbor-joining method.

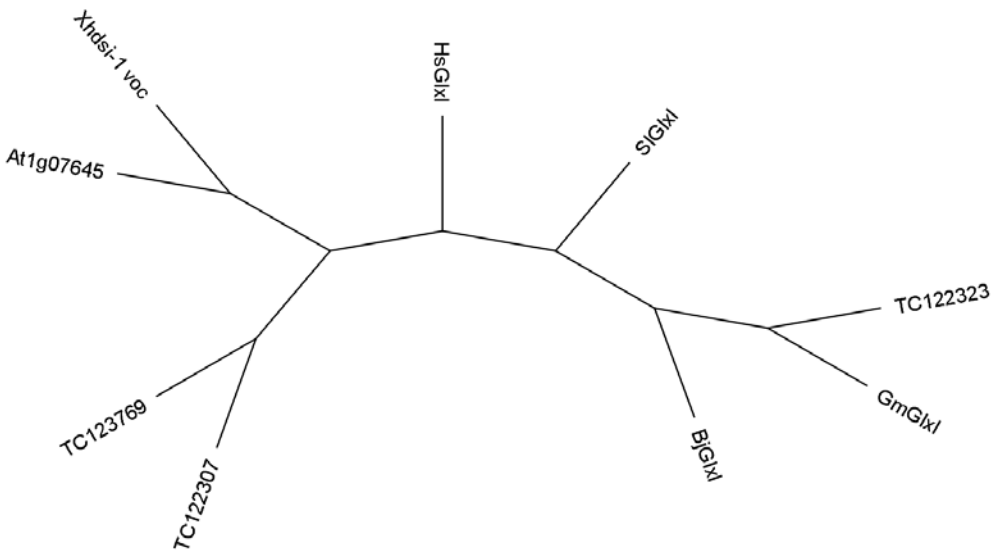

Figure 12. Transcript abundance in leaves following long-term salt application. Twenty-day-old plants were exposed to 50 mM NaCl for the first 24 hrs and 100 mM afterwards. We applied water (H_2O) as a control. Leaf samples from two plants per genotype were collected 3 days and 1 week after initial application. Total RNA (15 μg) was extracted and loaded in each lane, separated on an agarose-formaldehyde gel and transferred to a nylon membrane for hybridization. RNA was hybridized with the indicated radioisotope-labeled probe.

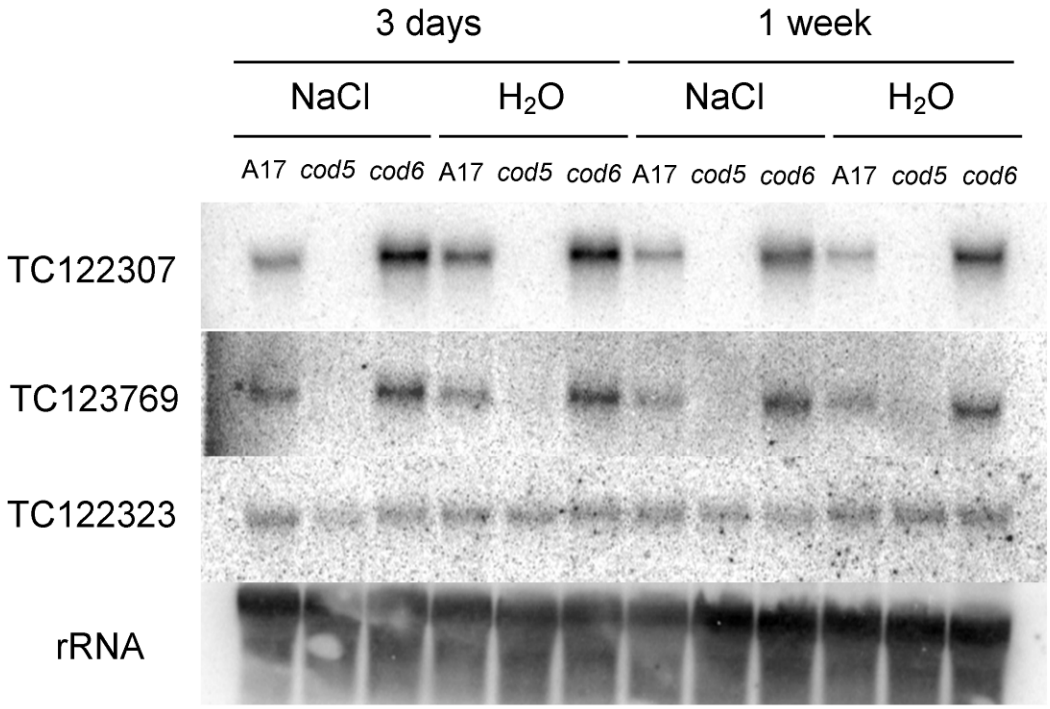

Figure 13. Semi-quantitative RT-PCR analysis of mRNA transcript abundance of glyoxalase I-like genes TC122307, TC123769 and TC122323 in leaf tissue of A17, *cod*5, and *cod*6. Alpha tubulin (Mtαtubulin) was used as a housekeeping gene.

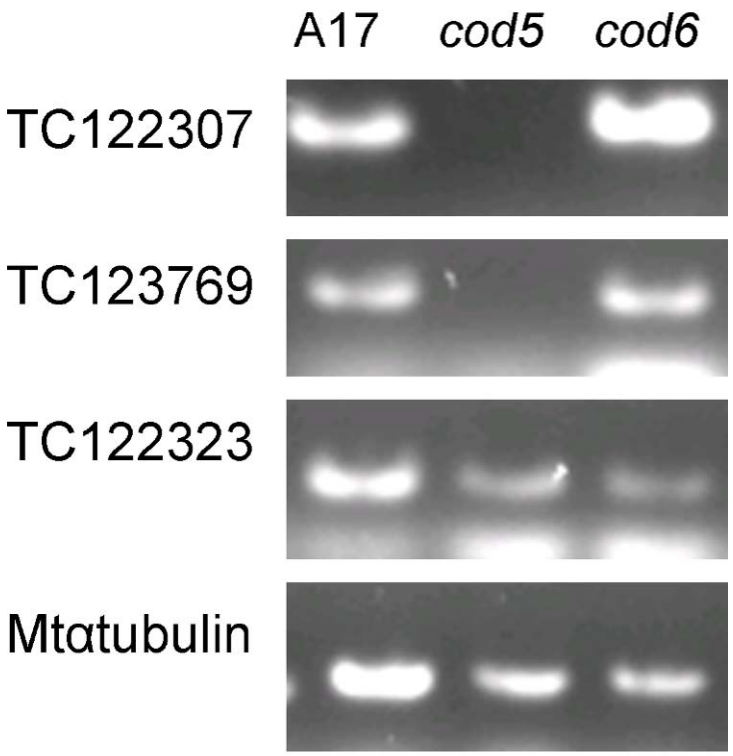

Figure 14. Transcript abundance in leaves following different types of salt treatment. Three plants per genotype were subjected to each treatment. Five-week-old plants were exposed to 50 mM NaCl for the first 24 hrs and 100 mM afterwards 48 and 72 hrs of first application. Other plants were subjected to 50 mM $CaCl_2$ or water (H_2O) for 72 hrs (conditions were as described in Fig. 2).

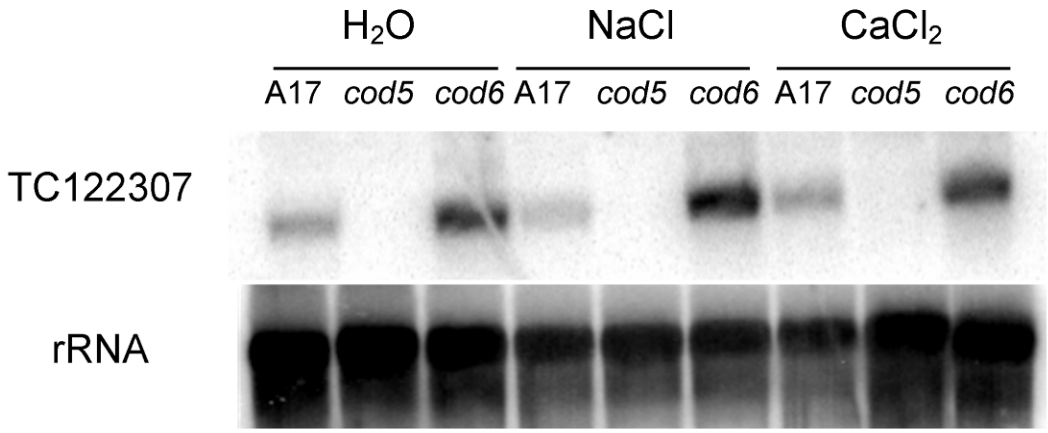

Figure 15. Schematic representation of the overexpression construct in pCAMBIA2300s vector. The expression of TC122307 is driven by the constitutive promoter CaMV35s and Kanamycin is used for plant selection.

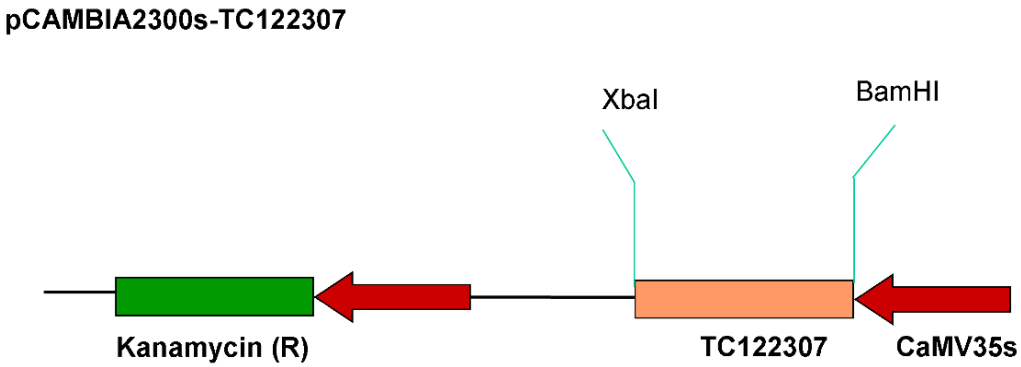

Figure 16. Electrophoresis of PCR product amplified from cDNA using primers designed to amplify the open reading frame of TC122307. Lane M, shows 100 bp DNA ladder. Arrow indicates the 646 bp band.

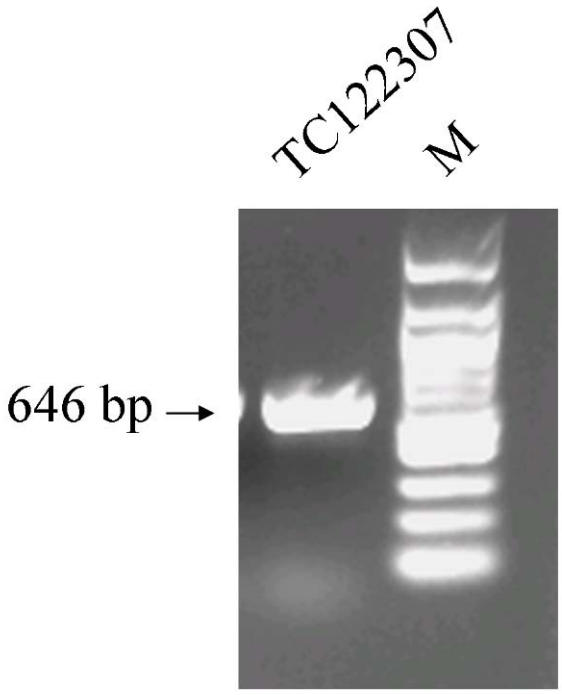

Figure 17. Electrophoresis of restriction digestion reactions of TC122307 (cut insert) and pCAMBIA2300s (cut vector) with BamHI and XbaI restriction enzymes. Lane M, shows 1 Kb DNA ladder. The arrows indicate the approximate size of the bands.

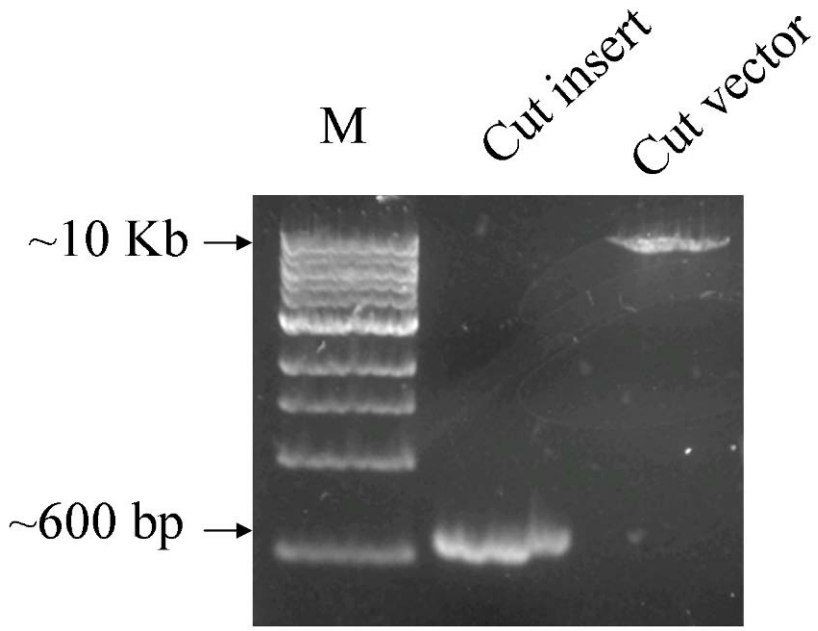

Figure 18. Electrophoresis of digestion reaction of pCAMBIA2300s/TC122307 with BamHI and XbaI to confirm presence of the transgene TC122307. Lane M, shows 1 Kb DNA ladder. Arrows indicate the vector and insert.

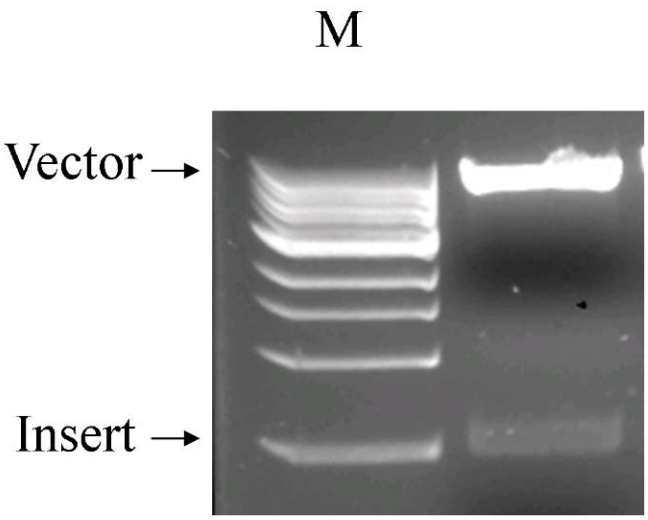

Figure 19. Electrophoresis of PCR products amplified from the indicated plasmid DNA template (pCAMBIA2300s, pCAMBIA/TC122307-1 and pCAMBIA/TC122307-2) with primers complementary to pCAMBIA2300s and the insert TC122307 in the case of pCAMBIA2300s/TC122307 -1 and -2. The plasmid alone (pCAMBIA2300s) was amplified with primers complementary the plasmid. Lane M, shows a 1 Kb DNA ladder. Smaller bands were amplified from pCAMBIA2300s/TC122307 -1 and -2 compared with PCR product from vector alone.

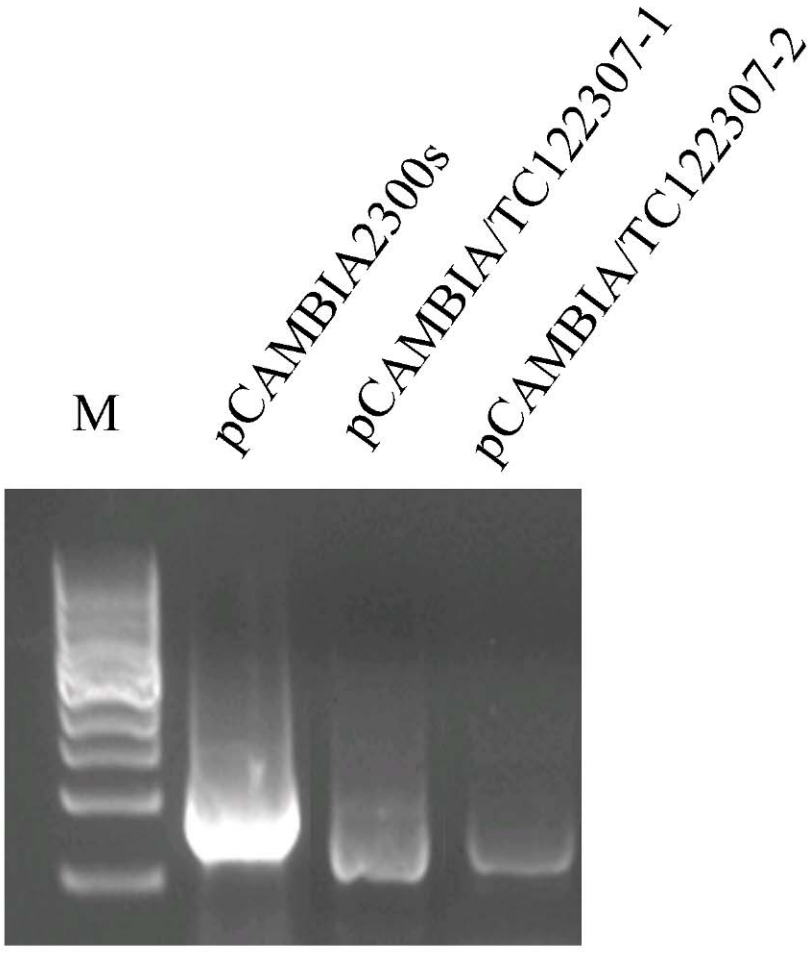

Table 4. List of primers used for semi-quantitative RT-PCR.

TC No.	Name or tentative annotation	GenBank Accession No.	Forward	Reverse
TC122307	Lactoylglutathione lyase	GT138749	CCT ATG AGT GAA TCA CGA CCC	GAA GCA GAA GAG ATG GGA ACT
TC123769	Lactoylglutathione lyase	AJ498324	GTG TCT CTC TTG TGT AGA TCA GTG	AAG AAG CAG TGC ATG AAG AA
TC122323	Lactoylglutathione lyase	GT140649	GAG GAT ACA TCT GAA GCT CCA AGT AAC	GCA GCA CTT CCT GTT ACA TTT CCA A
TC120531	Alpha tubulin	ES613496	CTC TGC TGA GAA GGC TTA TCA TG	AAG ATC CTC ACG GGC TTC AG

Table 5. List of primers used to make the overexpression constructs.

Primer name	Sequence
TC122323-BamHI	ATC ACA AGG ATC CAC CGA TTC GTA GA
TC122323-XbaI	GCA GTG ACC CGA TTC TAG ATG AAG G
TC122307-BamHI	GAG TGA AGG ATC CTA AGG GA
TC122307-XbaI	CAC CAC CAT ATT TCT AGA TTA ATA TG
pCAMBIA Forw	TAT GCT TCC TGC AGG TAT GTT GTG TG
pCAMBIA Rev	CTC TTA GGT GAG CTC GCC AAT ATA TCC T

REFERENCES

Al-Khatib M, McNeilly T and Collins JC (1993) The potential of selection and breeding for improved salt tolerance in lucerne (*Medicago sativa* L.). Euphytica 65: 43-51

Armstrong RN (2000) Mechanistic diversity in a metalloenzyme superfamily. Biochem 39: 13625-13632

Aronsson AC, Tibbelin G and Mannervik B (1979) Purification of glyoxalase I from human erythrocytes by the use of the affinity chromatography and separation of the three isoenzymes. Anal Biochem 92: 390-393

Aydi S, Sassi S and Chedly A (2008) Growth, nitrogen fixation and ion distribution in *Medicago truncatula* subjected to salt stress. Plant Soil 312: 59-67

Babbitt PC and Gerlt JA (1997) Understanding enzyme superfamilies. J Biol Chem 272: 30591-30594

Bagga S, Das R and Sopory SK (1987) Inhibition of cell proliferation and glyoxalase-I activity by calmodulin inhibitors and lithium in *Brassica oleracea*. J Plant Physiol 129: 149-153

Benedito VA, Torrez-Jerez I, Murray JD, et al (2008) A gene expression atlas of the model legume *Medicago truncatula*. Plant J 55: 504-513

Bernstein L and Hayward HE (1958) Physiology of salt tolerance. Annu Rev Plant Physiol 9: 25-46

Bernstein L (1975) Effects of salinity and sodicity on plant growth. Annu Rev Phytopathol 13: 295-312

Briskin DP (1990) Ca^{2+} translocating ATPase of the plant plasma membrane. Plant Physiol 94: 397-400

Bryson K, McGuffin LJ, Marsden RL, Ward JJ, Sodhi JS and Jones DT (2005) Protein structure prediction servers at University College London. Nucl Acids Res: 33 (Web Server issue) W36-38.

Bush DS (1995) Calcium regulation in plant cells and its role in signaling. Annu Rev Plant Physiol Plant Mol Biol 46: 95-122

Chakravarty TN and Sopory SK (1998) Blue light stimulation of cell proliferation and glyoxalase I activity in callus cultures of *Amaranthus paniculatus*. Plant Sci 132: 63-69

Chen F, Wollmer MA, Hoerndli F, et al (2004) Role for glyoxalase I in Alzheimer's disease. Proc Natl Acad Sci U S A 101: 7687-7692

Church GM and Gilbert W (1984) Genomic sequencing. Proc Natl Acad Sci U S A 81: 1991-1995

Clarkson DT, Brownlee C and Ayling SM (1988) Cytoplasmic calcium measurements in intact higher plant cells: results from fluorescence ratio imaging of Fura-2. J Cell Sci 91: 71-80

Clough SJ and Bent AF (1998) Floral dip: a simplified method for *Agrobacterium*-mediated transformation of *Arabidopsis thaliana*. Plant J 16: 735-743

Collier R, Fuchs B, Walter N et al. *Ex vitro* composite plants: an inexpensive, rapid method for root biology. Plant J 43: 449-457

Cook DR (1999) *Medicago truncatula* - a model in the making! Curr Opin Plant Biol 2: 301-304

de Lorenzo L, Merchan F, Laporte P, et al (2009) A novel plant leucine-rich repeat receptor kinase regulates the response of *Medicago truncatula* roots to salt stress. Plant Cell 21: 668-680

Drummond AJ, Ashton B, Buxton S, Cheung M, Cooper A, Heled J, Kearse M, Moir R, Stones-Havas S, Sturrock S, Thierer T and Wilson A (2010) Geneious Basic. 5.0.3

Espartero J, Sanchez-Aguayo I and Pardo JM (1995) Molecular characterization of glyoxalase-I from a higher plant; upregulation by stress. Plant Mol Biol 29: 1223-1233

Franceschi VR and Nakata PA (2005) Calcium oxalate in plants: formation and function. Annu Rev of Plant Biol 56: 41-71

Franceschi VR and Horner HTJr (1980) Calcium oxalate crystals in plants. Bot Rev 46: 361-419

Geisler M, Axelsen KB, Harper JF, et al (2000) Molecular aspects of higher plant P-type Ca^{2+}-ATPases. BBA - Biomembranes 1465: 52-78

Goffard N and Weiller G (2007) GeneBins: a database for classifying gene expression data, with application to plant genome arrays. BMC Bioinformatics 8: 87

Hernández JA, Olmos E, Corpas FJ, et al (1995) Salt-induced oxidative stress in chloroplasts of pea plants. Plant Sci 105: 151-167

Hoque MA, Banu MNA, Nakamura Y, et al (2008) Proline and glycinebetaine enhance antioxidant defense and methylglyoxal detoxification systems and reduce NaCl-induced damage in cultured tobacco cells. J Plant Physiol 165: 813-824

Ilarslan H, Palmer RG and Horner HT (2001) Calcium oxalate crystals in developing seeds of soybean. Ann Bot 88: 243-257

Inoue Y, Tsujimoto Y and Kimura A (1998) Expression of the glyoxalase I gene of *Saccharomyces cerevisiae* is regulated by high osmolarity glycerol mitogen-activated protein kinase pathway in osmotic stress response. J Biol Chem 273: 2977-2983

Jain M, Choudhary D, Kale RK, et al (2002) Salt-and glyphosate-induced increase in glyoxalase I activity in cell lines of groundnut (*Arachis hypogaea*). Physiol Plant 114: 499-505

Kim MC, Chung WS, Yun D, et al (2009) Calcium and calmodulin-mediated regulation of gene expression in plants. Mol Plant 2: 13-21

Kok DJ, Blomen LJMJ, Westbroek P, et al (1986) Polysaccharide from coccoliths ($CaCO_3$ biomineral). Eur J Biochem 158: 167-172

Korth KL, Doege SJ, Park S, et al (2006) *Medicago truncatula* mutants demonstrate the role of plant calcium oxalate crystals as an effective defense against chewing insects. Plant Physiol 141: 188-195

Libert B and Franceschi RV (1987) Oxalate in crop plants. J Agric Food Chem 35: 926-938

Lin F, Xu J, Shi J, et al (2010) Molecular cloning and characterization of a novel glyoxalase I gene TaGly in wheat *(Triticum aestivum* L.). Mol Biol Rep 37: 729-735

Mannervik B and Ridderstrom M (1993) Catalytic and molecular properties of glyoxalase I. Biochem Soc Trans 21: 515-517

McLellan AC, Thornalley PJ, Benn J, et al (1994) Glyoxalase system in clinical diabetes mellitus and correlation with diabetic complications. Clin Sci 87: 21-29

McNair JB (1932) The interrelation between substances in plants: essential oils and resins, cyanogen and oxalate. Am J Bot 19: 255-272

Merchan F, Crespi M and Frugier F (2007) Response of *Medicago truncatula* to salt stress. *Medicago truncatula* handbook. p 13-16

Mulako I, Farrant JM, Collett H, et al (2008) Expression of Xhdsi^{-1VOC}, a novel member of the vicinal oxygen chelate (VOC) metalloenzyme superfamily, is up-regulated in

leaves and roots during desiccation in the resurrection plant *Xerophyta humilis* (Bak) Dur and Schinz. J Exp Bot 59: 3885-3901

Nakata PA and McConn MM (2000) Isolation of *Medicago truncatula* mutants defective in calcium oxalate crystal formation. Plant Physiol 124: 1097-1104

Nakata PA and McConn MM (2003) Calcium oxalate crystal formation is not essential for growth of *Medicago truncatula*. Plant Physiol Bioch 41: 325-329

Nakata PA and McConn M (2007) Isolated Medicago truncatula mutants with increased calcium oxalate crystal accumulation have decreased ascorbic acid levels. Plant Physiol Bioch 45: 216-220

Niu X, Bressan RA, Hasegawa PM, et al (1995) Ion homeostasis in NaCl stress environments. Plant Physiol 109: 735-742

Nomenclature Committee of the International Union of Biochemistry (NC-IUB) (1979) Units of Enzyme Activity. Eur J Biochem 97: 319-320

Palta JP (1990) Leaf chlorophyll content. Rem Sens Rev 5: 207-213

Parida AK and Das AB (2005) Salt tolerance and salinity effects on plants: a review. Ecotoxicol Environ Safe 60: 324-349

Pitman M and Läuchli A (2004) Global impact of salinity and agricultural ecosystems. Salinity: environment - plants - molecules. Kluwer Academic Publishers, Netherlands, p 3-20

Qudeimat E, Faltusz AMC, Wheeler G, et al (2008) A PIIB-type Ca2+-ATPase is essential for stress adaptation in *Physcomitrella patens*. Proc Natl Acad Sci U S A 105: 19555-19560

Ramaswamy O, Pal S, Guha-Mukherjee S, et al (1984) Correlation of glyoxalase I activity with cell proliferation in *Datura callus* culture. Plant Cell Rep 3: 121-124

Roberts DM and Harmon AC (1992) Calcium-modulated proteins: Targets of intracellular calcium signals in higher plants. Annu Rev Plant Physiol Plant Mol Biol 43: 375-414

Roy SD, Saxena M, Bhomkar SP, et al (2008) Generation of marker free salt tolerant transgenic plants of *Arabidopsis thaliana* using the gly I gene and cre gene under inducible promoters. Plant Cell Tiss Organ Cult 95: 1-11

Rulli A, Carli L, Romani R, et al (2001) Expression of glyoxalase I and II in normal and breast cancer tissues. Breast Cancer Res Tr 66: 67-72

Sambrook J and Russell DW (2001) Molecular cloning: a laboratory manual. Cold Spring Harbor Laboratory Press, Cold Spring Harbor, New York

Schnoes AM, Brown SD, Dodevski I, et al (2009) Annotation error in public databases: Misannotation of molecular function in enzyme superfamilies. PLOS Comput Biol 5: e1000605

Singla-Pareek SL, Yadav SK, Pareek A, et al (2008) Enhancing salt tolerance in a crop plant by overexpression of glyoxalase II. Transgenic Res 17: 171-180

Singla-Pareek SL, Reddy MK and Sopory SK (2003) Genetic engineering of the glyoxalase pathway in tobacco leads to enhanced salinity tolerance. Proc Natl Acad Sci U S A 100: 14672-14677

Singla-Pareek SL, Yadav SK, Pareek A, et al (2006) Transgenic tobacco overexpressing glyoxalase pathway enzymes grow and set viable seeds in zinc-spiked soils. Plant Physiol 140: 613-623

Skipsey M, Andrews CJ, Townson JK, et al (2000) Cloning and characterization of glyoxalase I from soybean. Arch Biochem Biophys 374: 261-268

Sommer A, Fischer P, Krause K, et al (2001) A stress-responsive glyoxalase I from the parasitic nematode *Onchocerca volvulus*. Biochem J 353: 445-452

Sunkar R, Bartels D and Kirch HH (2003) Overexpression of a stress-inducible aldehyde dehydrogenase gene from *Arabidopsis thaliana* in transgenic plants improves stress tolerance. Plant J 35: 452-464

Teakle NL and Tyerman SD (2010) Mechanisms of Cl^- transport contributing to salt tolerance. Plant Cell Environ 33: 566-589

Thornalley PJ (1990) The glyoxalase system: new developments towards functional characterization of a metabolic pathway fundamental to biological life. Biochem J 269: 1-11

Umeda M, Hara C, Matsubayashi Y, Li H, et al (1994) Expressed sequence tags from cultured cells of rice (*Oryza sativa* L.) under stressed conditions: analysis of transcripts of genes engaged in ATP-generating pathways. Plant Mol Biol 25: 469-478

Valencia R, Chen P, Ishibashi T, et al (2008) A rapid and effective method for screening salt tolerance in soybean. Crop Sci 48: 1173-1179

Veatch ME, Smith SE and Vandemark G (2004) Shoot biomass production among accessions of *Medicago truncatula* exposed to NaCl. Crop Sci 44: 1008-1013

Veena, Reddy VS and Sopory SK (1999) Glyoxalase I from *Brassica juncea*: molecular cloning, regulation and its over-expression confer tolerance in transgenic tobacco under stress. The Plant J 17: 385-395

Verdoy D, Coba de la Peña, T., Redondo FJ, et al (2006) Transgenic *Medicago truncatula* plants that accumulate proline display nitrogen-fixing activity with enhanced tolerance to osmotic stress. Plant Cell Environ 29: 1913-1923

Vinocur B and Altman A (2005) Recent advances in engineering plant tolerance to abiotic stress: achievements and limitations. Curr Opin Biotechnol 16: 123-132

Wang W, Vinocur B and Altman A (2003) Plant responses to drought, salinity and extreme temperatures: towards genetic engineering for stress tolerance. Planta 218: 1-14

Webb MA (1999) Cell-mediated crystallization of calcium oxalate in plants. Plant Cell 11: 751-761

Wimmers LE, Ewing NN and Bennett AB (1992) Higher plant Ca^{2+}-ATPase: primary structure and regulation of mRNA abundance by salt Proc Natl Acad Sci U S A 89: 9205-9209

Yadav SK, Singla-Pareek SL, Reddy MK, et al (2005a) Methylglyoxal detoxification by glyoxalase system: a survival strategy during environmental stresses. Physiol Mol Biol Plants 11: 1-11

Yadav SK, Singla-Pareek SL, Ray M, et al (2005b) Methylglyoxal levels in plants under salinity stress are dependent on glyoxalase I and glutathione. Biochem Biophys Res Commun 337: 61-67

Yamaguchi T and Blumwald E (2005) Developing salt-tolerant crop plants: challenges and opportunities. Trends Plant Sci 10: 615-620

Young ND and Udvardi M (2009) Translating *Medicago truncatula* genomics to crop legumes. Curr Opin Plant Biol 12: 193-201

Zhang HX and Blumwald E (2001) Transgenic salt-tolerant plants accumulate salt in foliage but not in fruit. Nat Biotechnol 19: 765-768